Chapter 3
Recognition-Based on Eye Biometrics: Iris and Retina

Josef Hájek and Martin Drahanský

1 Introduction

In today's security world, biometrics is an interesting and important approach. Ideally, the user interacts with a simple interface, and in a matter of seconds, the biometric system scans the biometric characteristic, whether it is fingerprint or eye iris, and decides whether the user is allowed to pass or not.

This work is focused on the way of scanning and processing the features of a human eye for biometric and biomedical purposes. The features are iris and retina, as they include enough unique information that by its range covers a set bigger than the current human population on Earth.

However, such systems are not perfect, and there is always room for improvement. Recently, it has been discovered that a viable course of the future of biometrics may lie in multimodal biometric systems, which combine more than one source of biometric information for evaluation (such as fingerprint and palm veins), unlike unimodal biometric systems, which only use one.

Biometry applies to different parts of the human body. If the part is damaged or removed altogether, further identification using this biometric is not possible. From all possible affections of our senses, loss of vision has the biggest impact on a person's everyday life. This impact is higher than a loss of memory, voice, or hearing, because 80% of all sensory information that human brain receives comes through our vision. The interesting fact is that a vast majority of visual losses can be prevented by an early recognition and diagnosis of the illness and its treatment. Visiting ophthalmologist can be stressful for some people not only because of fear of the examination itself but also, for example, because of a lack of time. This could be

J. Hájek · M. Drahanský (✉)
Brno University of Technology, Centre of Excellence IT4Innovations,
Brno 62166, Czech Republic
e-mail: drahan@fit.vutbr.cz

M. S. Obaidat et al. (eds.), *Biometric-Based Physical and Cybersecurity Systems*,
https://doi.org/10.1007/978-3-319-98734-7_3

at least partially solved by automated devices, which could evaluate the current patient's condition without any human intervention and possibly even determine anamnesis.

Relatively, lots of iris scanning and recognition algorithms exist. Devices are working, usable in practice, with compact dimensions and quite a good price. Its disadvantage is its inability to detect life and thus its easy fraudulence by, e.g., specially tailored contact lens, etc. For an area of high-security level, the iris is not recommended. If we now focus on eye retina, there is currently no existing biometric system that would be based on this modality. Eye retina has its disadvantages in more difficult scanning form, which is, however, an advantage for liveness detection, in bigger degree user cooperation and higher cost of the device; on the other hand, the possibility of creating fake eye retina is very low (nearly impossible), and also eye retina possesses relatively lot of stable features that can be used for recognition of a big number of people. If we think about the possibility of mixing these two biometric characteristics into one multimodal biometric system, we come to a clear view that the combination has its purpose because the current trends of biometric systems lead toward multimodal biometrics. That kind of device, which would combine eye retina and iris, currently does not exist on the market neither does it exist in any functional concept which would enable using this technology in practice.

We also cannot omit medical (or biomedical) applications, where ophthalmoscopes and fundus cameras are used. These are very expensive; they also do not enable automatic eye retina scanning. The iris is not very interesting for medical use – in eye retina, much more diseases are visible. We can also say that there is no useful expert system on the market which would enable an automatic detection and recognition of diseases that show up in eye retina. When designing and constructing a solution that would fulfill the criteria mentioned, it is necessary to consider these:

- User acceptance (fear of users from its usage).
- Amount of cooperation of user and device necessary.
- Quality of captured images.
- Scanning and processing time.
- Overall price of device and associated software.

Creating a complex and sufficiently robust device is also possible covering the requirements of both biometric and medical segments. The same device with small modifications can be used in both areas, while the only significant change would be software which in biometric systems would extract biometric features with a task of comparing these features with a saved pattern in a database; and in medical systems, it would build an image of the eye retina and would also save the iris; however the expert system would focus mainly on the detection of diseases and suggest possible diagnoses, which would make the ophthalmologist's job easier.

2 Anatomy of the Eye

The human eye is a unique organ which reacts to light and similar to other parts of the body can be used for biometric recognition purposes such as fingerprints, hand veins and geometry, face, etc. In the eye, there are two crucial parts which have relatively high biometric entropy and thus are very suitable for recognition. The first one is the iris, i.e., the colored front part of the eye. The second one is the retina which is responsible for light sensing and cannot be observed by the naked eye because it is located on the back side of the eyeball. Both of them are very well protected against physical damage because they are inner structures of the eye. Iris and retina biometric patterns are unique for each individual although, e.g., the color of the iris is genetically dependent (also applies for monozygotic twins). The base anatomy of the human eye is described in Fig. 3.1.

The human eye consists from [2]:

- *Transparent crystalline lens* is located immediately behind the iris. It is composed of fibers that come from epithelial (hormone-producing) cells. It acts to fine-tune the focusing of the eye.
- *Ciliary body* extends from the iris and connects to the choroid. This annular structure produces aqueous humor, holds the intraocular lens in a place, and also has a supporting function during eye accommodation.
- *Iris* is colored annular structure regulating pupil diameter and thus amount of light coming into the eye. Eye color is defined by the iris.

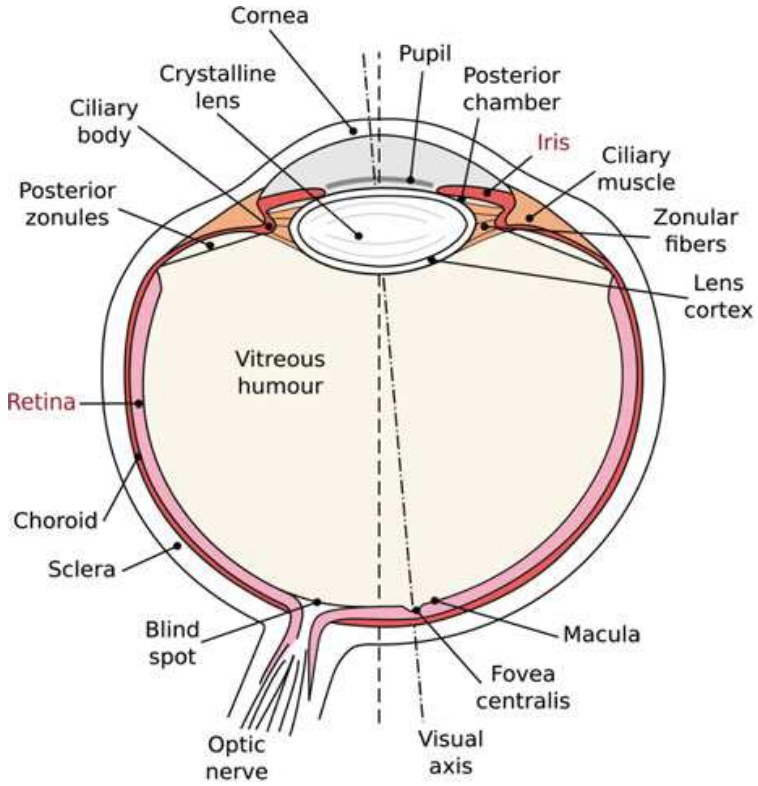

Fig. 3.1 Eye anatomy. (Modified from [1])

- *Pupil* is a hole located in the center of the iris. For an external observer, it seems to be a small black spot because light coming through the pupil into the eye is absorbed by biological tissues inside the eye.
- *Cornea* acts as a window of the eye. It is a transparent front surface of the eye covering the iris and the pupil admitting light into the eye.
- *Posterior chamber* contains aqueous humor and is located behind the peripheral part of the iris and in front of the suspensory ligament of the lens.
- *Ciliary muscle* is a ring of tiny muscles enabling changes in lens shape and thus controlling eye accommodation at varying distances. The muscles affect zonular fibers in the eye. When the muscles contract, they pull themselves forward and move the front lens part toward the axis of the eye.
- *Zonular fibers* are connections of the ciliary body and the crystalline lens which suspend in position during eye accommodation.
- *Lens cortex* is a part of lens comprising secondary lens fibers (long, thin, transparent cells, form the bulk of the lens).
- *Posterior zonules* pull the ciliary body, anterior zonules, and lens into the unaccommodated form.
- *Vitreous humor* is a transparent gelatinous mass filling the interior space of the eye. It contains no blood vessels, and more than 98% of its volume is water.
- *Choroid* is the vascular layer of the eye. It lies between the sclera and retina and provides nourishment for the back of the eye.
- *Sclera* is the protective outer layer of the eye enclosing the eyeball except the part covered by the cornea.
- *Retina* is a nervous tissue layer covering the back of the eyeball. It consists large amount of light-sensitive cells in which stimulation of electrochemical reactions is initiated and electrical impulses are transmitted to the brain.
- *Blind spot* is a small area where the optic nerve comes into the eye. On this area, there are no photoreceptors; i.e., there is no sensitivity to light.
- *Fovea centralis* is a small central spot or pit in the center of the macula containing only cones (no rods) which ensure the most sensitive color vision.
- *Macula* is a small circle shape yellowish area containing a maximum number of light-sensitive cells, thus ensuring maximum visual acuity. It is made up of almost wholly retinal cones.
- *Optic nerve* carries electrical impulses from visual stimuli in the retina out of the eye.
- *Optical axis* is the direct line through the center of the cornea, pupil, lens, and the retina. Along this line, the sharpest focus is drawn when we look at an object.
- *Visual axis* is a visual line from the center of the pupil to the fovea. This axis gives the best color vision (because the fovea consists of high-density cones and no rods).

The human eye is the most complicated and one of the most important sense organs from all. From the physical point of view, it is a transparent biconvex optical system, which focuses the light rays onto the surface of the retina by the help of the cornea and eye lenses. The *cornea* is a front elastic part of the eye. It is transparent,

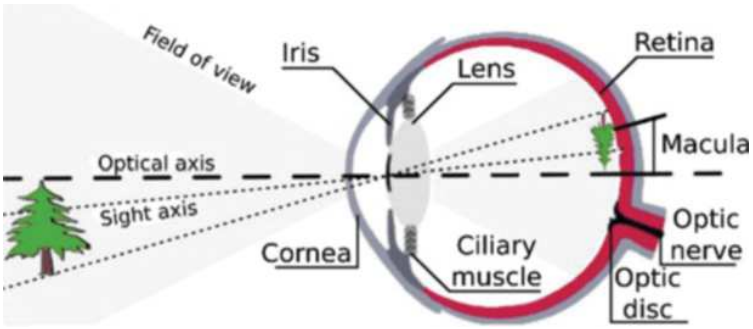

Fig. 3.2 Light projection into the eye

without vessels, and with the fixed optical power of more than 43 diopters represents approximately two-thirds of the eye's total power.

Another optic element of the eye is a *lens* with the ability to change its shape and thus optical power and focal length. It allows to focus on an object at various distances from the observer (eye accommodation). The minimal and maximal distance which the eye is able to focus on is given by two points [3]:

- *Near point* – the shortest distance between an object and the observer which still gives a sharp image on the retina. In this case, the optical system of the eye has the largest optical power of more than 60 diopters. A healthy eye is able to focus on the object at a distance of 25 cm without any exertion.
- *Far point* – the longest distance between an object and the observer which still gives a sharp picture on the retina. The eye lens has the lowest optical power. For a healthy individual, this distance is in infinity.

The light entering the eye is controlled by the *iris*. The surface of the iris has a shape of an annulus and is able to control the diameter of the pupil and thus the amount of light falling on the *retina*. It has a similar function as the aperture of a camera lens.

Fig. 3.2 shows the projection into the eye. The resulting image of the outside world is in the eye inverted (upside down), mirrored, and reduced. The captured image is subsequently transformed to electric signals which are directed to the brain via the optic nerve. In the brain, the image is processed, i.e., it is flipped upside down and mirrored according to the reality.

A thorough understanding of eye anatomy is closely related to a proposal of optical system for acquirement of digital copy of the eye that can be used for medical as well as for biometric purposes.

2.1 Anatomy of the Retina

As shown in Fig. 3.1, the *retina* is located on the back part of the inner surface of the eyeball. The retina is considered as part of the central nervous system and is the only one which can be observed noninvasively and directly. This light-sensitive tissue has a similar function like the film in a camera. Optical system within the eye focuses an

image onto the retina surface, initiating several electrical and chemical reactions. Nerve fibers in the retina transport these signals to the brain which interprets them as visual images.

Two types of photosensitive cells are contained in the retina – the rods and three different types of cones with sensitivity to various ranges of wavelengths; hence the cones enable us to distinguish miscellaneous colors. Only one type of rod is much more sensitive to light than cones, and that's the reason why we cannot recognize colors well in a dim light. A whole retina surface covers approx. 70% of the inner surfaces of the eyeball and contains approximately seven million cones and about 75–150 million rods.

On the retina, there are two most conspicuous structures (see Fig. 3.3) – *optic disc* (blind spot) and a *macula* (yellow spot). The optic disc is actually the head of an optic nerve entering the eye and is also a point where the blood vessels, supplying the retina, come into the eye. On colored fundus images, it has bright yellow or even white color. It has more or less a circular shape, which is interrupted by protruding vessels. Sometimes the shape can be elliptical, which is caused by the non-negligible angle between the level of image and level of the optical disc. The diameter is approx. 1.8 mm and is placed from 3 to 4 mm to the nasal side of the fovea. Optic disc completely lacks any light-sensitive cells, so if the light reaches this place, it cannot be visible for the person. In this case, the missing part of the object is completed by the brain (that is why it is also called *blind spot*). We can easily convince ourselves about the existence of blind spot. A test is shown in Fig. 3.4.

When observing the cross with the right eye while the left eye is closed, at a certain distance from the image, the black circle disappears. This is exactly the moment when the image is depicted on the optic disc.

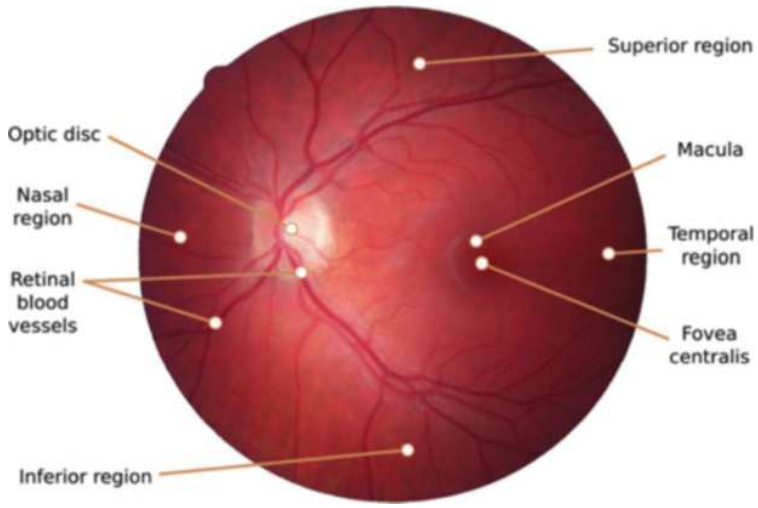

Fig. 3.3 Overview of the retina

Fig. 3.4 Blind spot test

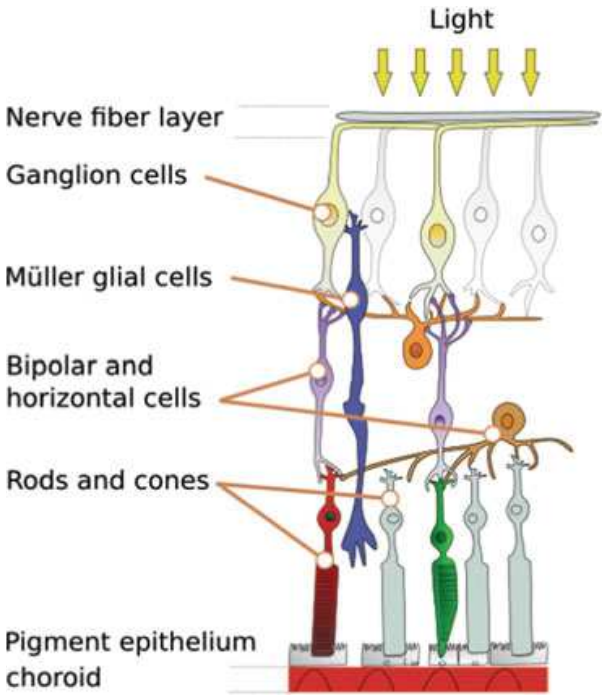

Fig. 3.5 Retinal layered structure. (Modified from [4])

On the other hand, the macula is an area of the sharpest vision. It has a circular shape with a diameter of approx. 5 mm and contains a high density of photosensitive cells, and cones predominate. In the fovea, there are cones only (no rods). Cells density decreases with distance from the macula to the rest surface of the retina. Interestingly, the name "yellow spot" is not derived from the color of the macula (which is rather dark red) but is according to its color observed in the eyes of dead people. The retina itself is a tissue with a thickness of 0.2–0.5 mm. It is described with several layers as shown in Fig. 3.5.

Light first passes through the optic fiber layer and the ganglion cell layer where the most amount of nourishing blood vessels is located. The light is transferred through the layer by Müller glial cells that act as optic fibers and then is received by the photoreceptor cells, cones, and rods which convert the light into the nerve impulses sent through the nerve fibers and optic nerve to the brain. The absorption of photons by the visual pigment of the photoreceptors is firstly translated into a biochemical message and then an electrical message stimulating all the appropriate neurons of the retina. Nourishment of the photoreceptor cells is ensured by the layer of retinal pigment epithelium cells which are fed by blood vessels in the choroid.

2.2 Anatomy of the Iris

The *iris* is a front colored part of the eye which is not hidden inside and can be observed by the naked eye. The annular shape with a central hole called pupil has the same functionality as an aperture of the photo camera – regulating the amount of light coming into the eye. The outer border of the iris is fixed, connected to the ciliary body, while the size of the pupil can vary depending on ambient light. The pupil is

not located exactly in the middle but is a little bit moved down and separates the anterior chamber from the posterior chamber. The pupil appears to be black because no light is coming from the eye.

On the back side of the iris lies heavily pigmented layer – epithelium – preventing excessive light from entering the eye. The pigment that gives the iris its color is called melanin. The amount of melanin gives the unique color of the iris. If less, long wavelengths of light are absorbed and short wavelengths are reflected; thus, the eye seems to be blue. On the other hand, more amount of melanin causes brown color [5].

The iris can be divided into pupillary zone and outer ciliary zone. The size of the pupillary zone is given by the maximal size of the extended pupil. These areas are separated by a meanderingcircular ridgeline called *collarette*. Pupillary margin is encircled by fibers of sphincter papillae muscle lying deeply inside the stroma layer. Contraction of the sphincter causes pupil constriction which subsequently results in so-called contraction furrows in the iris. The depth of these furrows depends on the dilation of the pupil caused by the action of the dilator muscle which belongs to the anterior epithelial layer. The dilator muscle fibers are arranged in a radial pattern ending at the root of the iris. Another artifact giving the iris its typical structure is *crypts* occurring adjacent to the collaret, and smaller crypts are located on the iris periphery. The surface of the iris comprises a relatively high amount of structural and circular furrows, pits, and contraction folds. All the described features contribute to a highly detailed iris pattern that is very diverse across human population. While some biometric traits change with age, the iris stops developing around the age of 2 years [6]. In the case of twins, iris recognition has an advantage over face recognition. Monozygotic twins may be nearly identical in terms of facial features, but their irises are highly likely to display several differences in texture.

It is also interesting to note that it was claimed that each area of the body is represented by a corresponding area and patterns, colors, and other characteristics in the iris of the eye. This technique is called *iridology* [122] and can be used to determine information about general health of the person. However, this practice has never been proven as a reliable medical examination method because it makes no anatomic or physiological sense, and well-controlled scientific evaluation of iridology has shown entirely negative results (Fig. 3.6).

3 Iris Recognition

Iris recognition is currently one of the most secure technologies for access control systems. Due to the fine and unique texture of the iris, the probability of having the same iris texture is around 1 in 10^{78} [7], thus ensuring sufficient coverage of the population. However, the fact that the iris is located visibly and it is possible to take a photo from a distance of some meters, the risk of the iris pattern copy and subsequent counterfeit is relatively high. Hence, there should always be some additional security mechanisms (e.g., liveness detection) for high-secured access control.

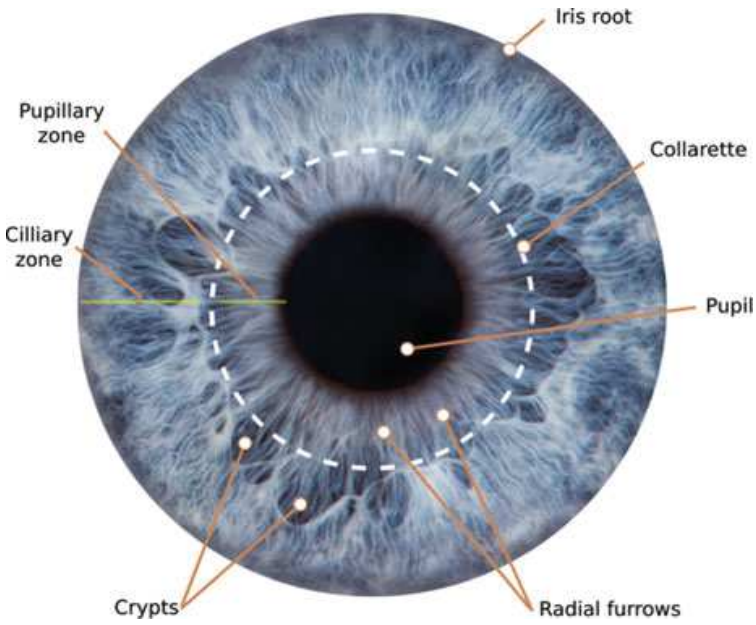

Fig. 3.6 Detailed iris anatomy

3.1 History of Iris Recognition

Although the patented and currently used algorithms have been introduced relatively recently, the concept behind iris recognition has a much longer history. The first idea about using pattern or coloration of the iris for recognition was published in 1886 by Alphonse Bertillon who mentioned in his work that "the features drawing of the areola and denticulation of the human iris" can be used for human recognition [8]. In 1936 the ophthalmologist Frank Burch proposed the concept of the method for individual recognition using iris patterns. However, since that time, it took more than six decades until two American ophthalmologists Dr. Leonard Flom and Dr. Aran Safir proposed and managed a patent for the iris identification concept in 1987. The concept was introduced, but they had no algorithms or implementation, and so their patent remained unrealized. Thus after 2 years, they approached Dr. John Daugman from Harvard University to develop algorithms for automatic and fast identification based on human iris. He formulated three characteristics which determine the iris as an ideal organ for recognition [9].

- It is an inner organ of the body very resistant to external influences.
- It is practically impossible to change its structure without causing eye damage.
- It is physiologically responsive to light, which allows to perform the natural liveness tests.

Dr. Daugman was awarded a patent for automated iris recognition in 1994. One year earlier, the Defense Nuclear Agency of the United States started to work on a prototype of iris recognition system which has been successfully completed and tested in 1995, thanks to the effort of doctors Flom, Safir, and Daugman. In the same year, the first commercial product became available [10]. The patented algorithms became widely licensed by several companies, and research on many aspects of this

technology and alternative methods has exploded to rapidly growing academic literature on related topics – optics, sensors, computer vision, security, etc.

3.2 Daugman's Algorithm

The algorithm invented by Dr. John Daugman was the first patented and subsequently deployed approach for automatic iris recognition system. It was the most significant milestone in iris recognition technology. Although patented more than 10 years ago, its principles are still used by some current iris recognition technologies.

The algorithm uses 2D Gabor wavelet transform. Each particular pattern on the iris is demodulated to obtain phase information for features extraction. Information is encoded into *iris code* bit stream, stored in databases allowing search at speeds of millions of iris patterns per second on a single CPU.

The first step of Gabor demodulation is locating the iris in the scanned picture. The iris must be scanned with high quality so that it can be mapped into phase diagrams containing the information about the iris position, orientation, and the number of specific identification attributes. It is then possible to compare it with the database using a pattern once the extraction is done. The principle of Daugman's algorithm is depicted in Fig. 3.7.

Firstly, the iris and its radius are located in the picture. It is done using the following operator [11]:

$$\max_{(r,x_0,y_0)} \left| G_\sigma(r) \frac{\partial}{\partial r} \oint_{r,x_0,y_0} \frac{I(x,y)}{2\pi r} ds \right| \tag{3.1}$$

where $G_\sigma(r)$ is Gaussian function of smoothing according to σ, $I(x,y)$ is the rough input picture, and the operator searches for the maximum in blurred partial

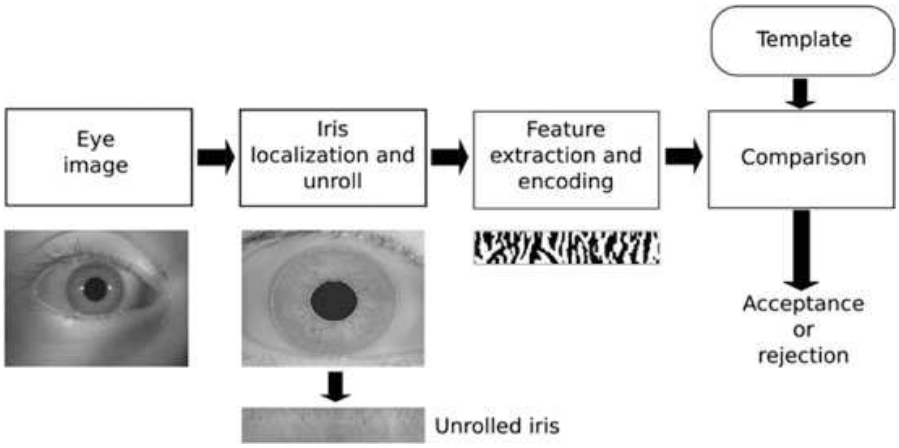

Fig. 3.7 Identification process according to Daugman's algorithm

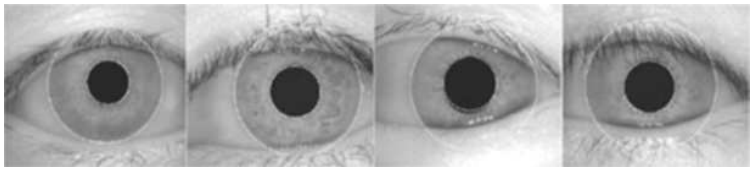

Fig. 3.8 Examples of located irises [12]

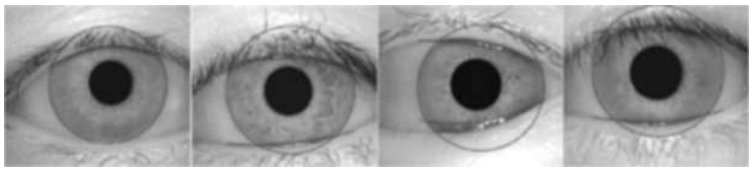

Fig. 3.9 Examples of located eyelids [13]

derivation with attention to radius r and middle coordinates (x_o, y_0). The operator is basically a circular edge detector and returns the maximum if the potential circle shares the middle of the pupil and the radius. Examples of located irises are shown in Fig. 3.8.

Another step is an eyelid localization. Using similar procedure as the one used when locating the iris – the exact position of the upper and the lower eyelid is found. Part of the previous formula used to detect the outline is changed from circular to arched, while parameters are set according to standard statistical methods of estimation so that they ideally correspond to each of the eyelid edges. Examples of located eyelids are shown in Fig. 3.9.

3.2.1 Daugman's Rubber Sheet Model

Daugman's rubber sheet model maps each point inside the iris into polar coordinates (r, θ), where r is in interval $\langle 0, 1 \rangle$ and θ is the angle in interval $\langle 0, 2n \rangle$.

This model compensates pupil dilatation and size inconsistency, thanks to the use of polar coordinates system which is invariant toward a size and translation. The model, however, does not compensate for rotational inconsistency, which is handled by the moving of the iris template in direction θ during comparison phase until both templates match together. Polar coordinate system usage is shown in Figs. 3.10 and 3.11.

3.2.2 Iris Features Encoding

Gabor filter in polar coordinate system is defined as [15]:

$$G(r, \theta) = e^{j\omega(\theta - \theta_0)} e^{-\frac{(r-r_0)^2}{\alpha^2}} e^{-\frac{(\theta-\theta_0)^2}{\beta^2}} \tag{3.2}$$

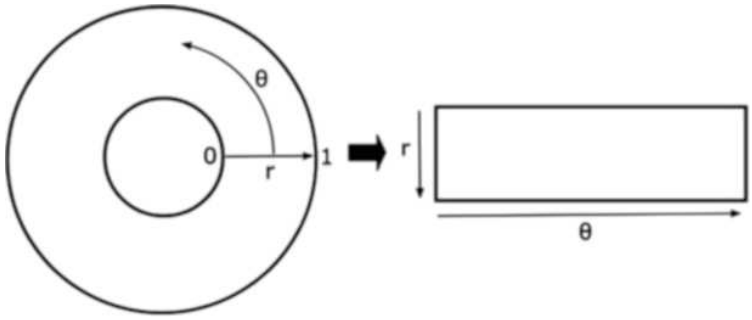

Fig. 3.10 Iris and pupil centers are coincident. (Modified from [14])

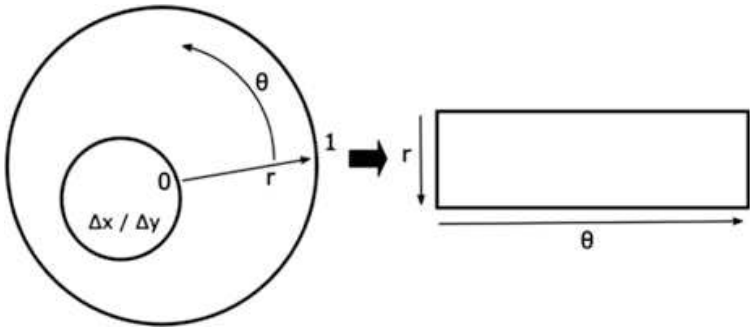

Fig. 3.11 Iris and pupil centers are not coincident. (Modified from [14])

where (r, θ) indicates the position in the picture, (α, β) defines effective height and length, and ω is filter's frequency. Demodulation and phase quantization are defined as [11]:

$$g_{\{Re,Im\}} = sgn_{\{Re,Im\}} \iint_{\rho\varnothing} I(\rho, \varnothing) e^{j\omega(\theta_0 - \varnothing)} e^{-\frac{(r_0-\rho)^2}{\alpha^2}} e^{-\frac{(\theta_0-\varnothing)^2}{\beta^2}} \rho d\rho d\varnothing \tag{3.3}$$

where $I(r, \phi)$ is the rough iris picture in polar coordinate system and $g_{\{\mathrm{Re,\,Im}\}}$ is a bit in the complex plane that corresponds to the signs of real and imaginary parts of the filter's responses. Illustration of the whole encoding process is shown in Fig. 3.12.

Iris' code contains 2048 bits – that is, 256 bytes. The size of input picture is 64 × 256 bytes, the size of iris' code is 8 × 32 bytes, and the size of Gabor filter is 8 × 8. An example of the encoded iris information contains Fig. 3.13.

3.2.3 Iris Codes Comparison

The comparison is done by calculating the Hamming distance between both 256-byte iris codes. Hamming distance between iris code A and B is defined as the amount of exclusive sums (XOR) between individual bits [9]:

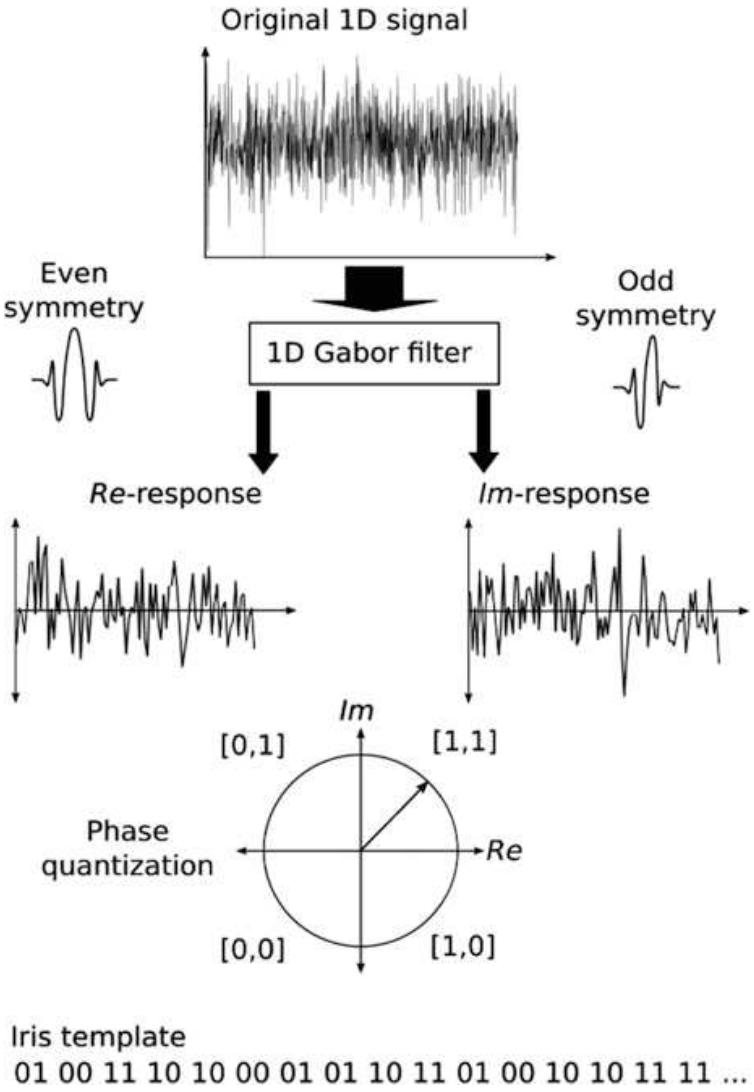

Fig. 3.12 Encoding process illustration. (Modified from [16])

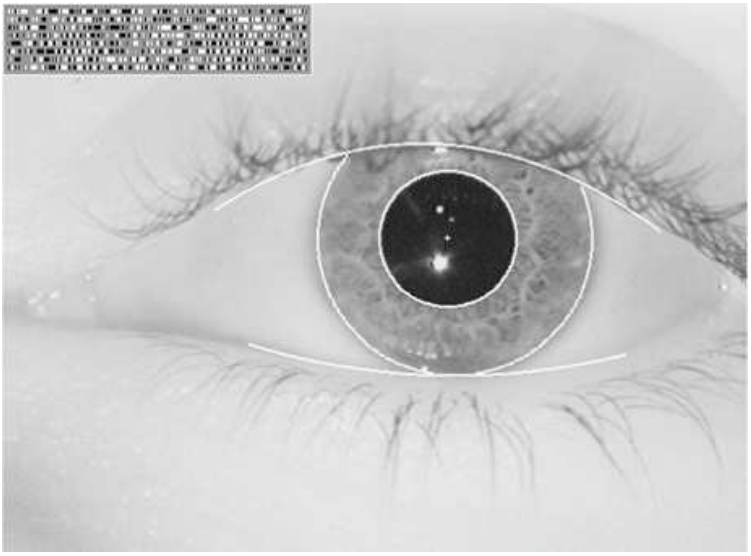

Fig. 3.13 Iris code example [11]

Fig. 3.14 Iris codes comparison

$$HD = \frac{1}{N} \sum_{j=1}^{N} A_j \otimes B_j \tag{3.4}$$

where $N = 2048$ (8×256), if the iris is not overshadowed by an eyelid. In that case, only valid areas are taken into consideration when calculating Hamming distance.

If both samples are obtained from the same iris, Hamming distance is equal or nearly equal to zero, thanks to high correlation of both samples. To ensure rotational consistency, one of the samples is shifted left or right, and each time the Hamming distance is calculated, the lowest Hamming distance is then considered as a final result of the comparison. An example of iris code comparison is shown in Fig. 3.14.

3.3 Characteristic of the Iris Recognition Technology

A selection of characteristics related to the suitability of iris recognition is listed below.

3.3.1 Acceptability

Acceptability of identification using the iris is on a middle level as no immediate interaction with the user is needed. The user only needs to stand in front of the device and look in the direction of the sensor from a given distance without moving his head. On the current devices, it takes approximately 2 s to scan and evaluate the picture of the user's iris. Systems for acquirement of irises on the fly (during walking) are in development, and first versions are available on the market. However these solutions have higher false to acquire rates, because the probability to get a high-quality iris sample during walking is lower in comparison with calmly staying cooperative user in front of the acquisition station.

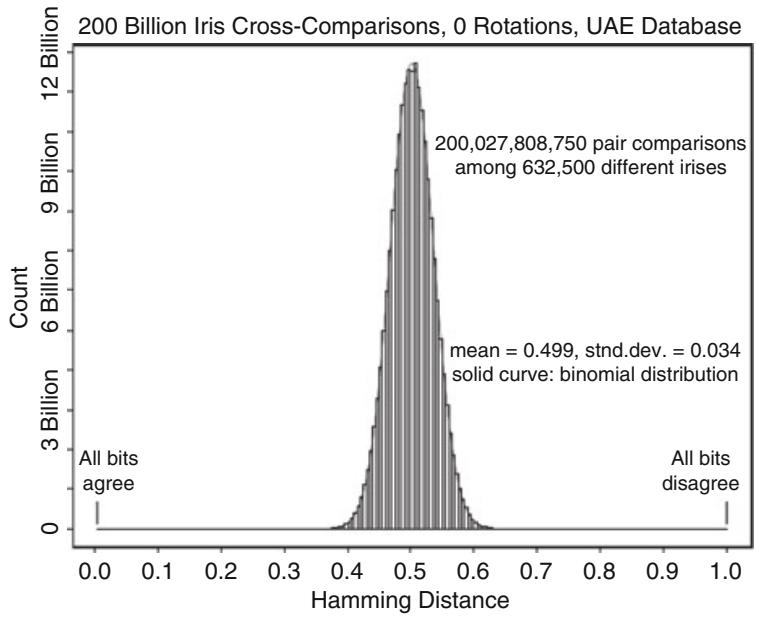

Fig. 3.15 Distribution of Hamming distance [17]

3.3.2 Reliability

During iris scan, insufficient information may be gotten because of ambient lighting, eyes not being open enough, and so on. However, it is relatively a reliable identification method.

The accuracy of the comparison of two iris samples is defined by the Hamming distance, that is, the number of bits that are different in both iris samples. For example, if the Hamming distance is 0.2, two irises differ by 20%. It is noted that a probability of incorrect comparison is 1:26,000,000, and Hamming distance of 0.32 (i.e., about 1/3 same bits from both samples) is sufficient.

Fig. 3.15 shows a distribution of Hamming distances when comparing big amount of irises [17]. The graph creates a binomial distribution with 50% probability (0.5). It also shows that it is highly improbable that two various irises could differ in less than 1/3 of information.

Table 3.1 shows the probabilities of false accept and false reject depending on the Hamming distance of two iris patterns. The Hamming distance value 0.342 is a point of equal error rate (ERR) where false accept and false reject rates are the same. This means that if the difference between currently scanned iris code record and one in the database is 34.2% or greater, they are considered to be from two different individuals.1.

3.3.3 Permanence

The iris is an internal organ and thus well protected but externally visible. Furthermore, the iris does not change with aging – one enrollment should be sufficient for a lifetime with the exception of damage due to accident or disease.

Table 3.1 Hamming distances and error rates probabilities [18]

Hamming distance	False accept probability	False reject probability
0.280	1 in 10^{12}	1 in 11,400
0.290	1 in 10^{11}	1 in 22,700
0.300	1 in 6.2 billion	1 in 46,000
0.310	1 in 665 million	1 in 95,000
0.320	1 in 81 million	1 in 201,000
0.330	1 in 11 million	1 in 433,000
0.340	1 in 1.7 million	1 in 950,000
0.342	1 in 1.2 million	1 in 1.2 million
0.350	1 in 295,000	1 in 2.12 million
0.360	1 in 57,000	1 in 4.84 million
0.370	1 in 12,300	1 in 11.3 million

3.4 Advantages and Disadvantages of Iris Technology

Iris recognition is relatively new among other usual biometric methods; however, it has attracted attention from industry, from government, and also from the army due to its highly desirable properties for personal identification.

External visibility of the human retina ensures a relatively easy scan of its structure. On the other hand, some civil liberties campaigners have voiced concerns about privacy because the iris pattern can be captured from relatively long distance (up to tens of meters) without any cooperation and knowledge of the person.

3.4.1 Advantages

- *Pattern permanence* – iris pattern is well protected and stable through the whole life of an individual. It is not prone to external influences, unlike the face, hand, or fingers. However, the iris can still be affected by eye diseases like diabetes or some other serious disease causing alternations in the iris.
- Uniqueness – remarkable uniqueness of the iris is given by richness of texture details – crypts, coronas, stripes, furrows, etc. Even genetically similar people have totally different iris texture.
- *User-friendliness* – iris is an externally visible organ and enables scanning from distance without any close interaction with a sensor. It requires minimal cooperation with the user. It also makes the recognition more hygienic in comparison to touch-based biometrics such as fingerprint recognition.
- *Speed and scalability* – iris region images can be normalized into rectangular regions of fixed size; thus, fixed-length feature codes can be extracted extremely fast, and matching can be performed easily by the XOR operation. For this reason, the iris recognition is very suitable for large deployments with databases of thousands of users.

- *Relative simple liveness detection (anti-spoofing)* – is given by natural physiology of changing pupil size depending on ambient light or by eye movement called hippus [19].
- *Robustness* – iris recognition system is well resistant to changes in the external environment. For example, voice recognition cannot be processed properly with excessive background noise.

3.4.2 Disadvantages

- *Fear of eye damage* – one of the main disadvantages of using iris recognition system is that the user has to trust the system because sometimes it is said to be a harmful system when using it for a longer period of time because the iris is constantly being scanned by infrared light.
- *Price* – e.g., widely used fingerprint recognition is much cheaper in general. However, iris recognition is still one of the most accurate biometrics, and the prices for devices are dropping down each year, because of increasing amount of installations worldwide.
- *Reliability* – iris recognition can be easily affected by the use of contact lenses or glasses, eyelashes, or reflection from the cornea, and this often results in false rejection of the user.
- *Security* – it can be quite easy to counterfeit an iris sensor. An attacker needs to have iris pattern obtained from a user (is possible to take iris picture from a distance without any user cooperation and awareness) and print the pattern or make a fake contact lenses. For better security, the system has to be equipped with liveness detection (anti-spoofing).

3.5 Related Standards

- *ANSI INCITS 379–2004: Information technology – Iris Image Interchange Format*. This standard describes the format for transmitting visual information about the iris. This includes attribute definition, data record and samples, and matching criteria.
- *ISO/IEC 19794–6:2011: Information technology – Biometric data interchange formats – Part 6: Iris image data*. This standard defines two alternative formats for data representation. The first is based on direct saving into uncompressed format, and the second one requires some preprocessing. However, data is compact and contains only information regarding the iris.

3.6 Commercial Applications and Devices

Many examples of practical usage do exist. These systems are most widespread in the United Arab Emirates, where they are used in airports and ports (c. 3.8 million comparisons daily). Another example can be the system at Schiphol Airport in the Netherlands used by people with high flight frequency. In Czech Republic, this system has not been deployed yet for a practical larger-scale application. Another noncritical example of use is at El Salvador sugar mill [20] where the clatter of time clocks has been replaced by a quiet time-and-attendance system based on iris recognition. The lines have been reduced and time fraud eliminated. In Afghanistan, UNHC (United Nations High Commission) uses iris recognition to control immigrants from surrounding countries.

Relatively large numbers of devices that are capable of iris recognition are currently available on the market. Some of them (just small selection) are mentioned below.

• BM–ET200/BM–ET330 (Panasonic)
Panasonic BM-ET200/BM-ET330 [21] offers small wall mounted recognition device able to enroll up to 5025 users depending on the mode the device is operating in. Templates are stored locally in ciphered internal memory. The number of users can be higher in the case of using Ethernet network deployment with database stored and maintained on the central server. Recognition time is 0.3 s with scanning distance of 30–40 cm. Supported operation modes are (a) 1:N – identification mode (one to many), (b) 1:1 – verification mode based on PROX Card or PIN input or iris data from local cache or server database, (c) 1:1 verification with smart card, and (d) standalone-built-in web server for enrollment (Fig. 3.16).

• IrisAccess 4000 (LG Electronics)
LG IrisAccess 4000 [22] offers iris recognition technology which can be easily integrated into current security systems through common Ethernet, USB, or serial connection, but local template database is not possible. The devices scan both irises, and a variety of authentication modes can be configured for the right, left, or both

Fig. 3.16 Panasonic BM-ET200 [21]

Fig. 3.17 IrisAccess 4000 [22]

eyes at the same time. Its optical system is also prepared for multi-biometric use allowing facial recognition. However, this has to be handled by external third-party application. Scanning distance is 25–37 cm and offers a standard "one-to-many" identification mode with identification time from 1 to 2 s (Fig. 3.17).

• iCAM D1000 (Iris ID)

Iris ID Systems, Inc., is the key developer and driver of the commercialization of iris recognition technology since 1997. The recognition system iCAM D1000 is the sixth generation, and thousands of them are deployed in different countries worldwide. It is a 1082 mm height wall mount device with autonomous positioning system for variously tall people. Straight interaction with the device is not required – scanning distance is 75 cm (±20 cm). It is able to capture the face and iris images in 2–3 s (dual capture) and transfer them to PC equipped with recognition software [23] (Fig. 3.18).

• BO 2120 EVM (Iritech, Inc.)

Another well-known player in the field of iris recognition technology is a company Iritech, Inc., offering monocular or binocular iris recognition devices and OEM modules ready to be integrated into existing product lines. An example of hardware module is an evaluation kit BO 2120 EVM [24]. It is a small monocular system working in near-infrared light spectrum with scanning distance of 5 cm and encrypted internal memory for up to 1000 iris templates. Matching query against full memory of templates is within less than 0.5 s. Available application programming interface for several programming languages allows fast integration into a new or into the current devices where is a requirement for iris recognition technology (Fig. 3.19).

Fig. 3.18 iCAM D1000 [23]

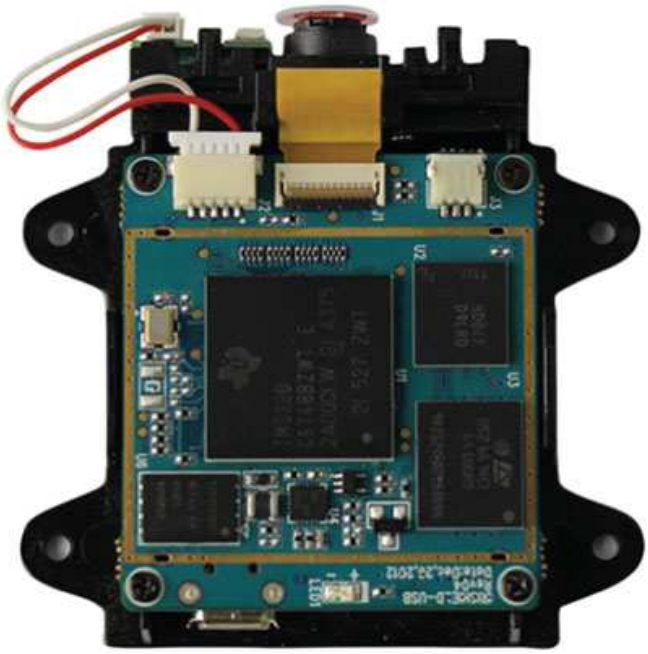

Fig. 3.19 Iritech BO 2120 [24]

4 Retinal Recognition

According to available information, the retina recognition is not currently used in practice at all. This is caused by several factors, e.g., complicated optical system, price, and low user-friendliness. Retinal recognition has clear advantages in

uniqueness and a number of features compared to other biometrics (up to 400), and also, it is the only place in the human body with the possibility to observe the blood vessels noninvasively and directly. Also, no standards for retinal recognition currently exist; however, it is basically the image of the blood vessels similar to the one used in the recognition using hand or finger blood vessels. Tests of the first constructed device for retinal recognition reported no false accepts and three-attempt false reject error rate (the user is rejected if a match is not found in three trials) of less than 1% [25]. Any counterfeit of the retinal recognition system is very difficult, because, in the first step, the attacker should get a retinal image, which is not possible without user cooperation and awareness. In the second step, the attacker would have to imitate an optical system of the eye so that the biometric system could perform a scan of the retinal fake.

Human recognition which uses the pattern of blood vessels on the back of the eyeball is a very specific branch of biometrics. Although retina-based technique of identification is often perceived as a very secure biometric approach, this method is not widely used due to a few major disadvantages. One of them is related to security. The retina is located inside on the back of the eye, and it is technically difficult and inconvenient to acquire the retinal image. The retina is not a visible part of the human body in comparison to the iris or face, which allows being captured even from longer distances. In this case, it is necessary to have an appropriate optical system which is able to focus the whole eye through the pupil and take a picture of the retinal part. This process leads to complicated and expensive optic device.

On the other hand, it is very hard to counterfeit such recognition because the attacker would have to obtain a retinal image from the relevant individual and simulate an optical system of the eye.

4.1 History of Retinal Recognition

In 1935, ophthalmologists Carleton Simon and Isidore Goldstein who have been exploring eye diseases have found out that the pattern of blood vessels of the retina is different and unique for each individual. They have subsequently published a paper about using retinal blood vessels pattern as a unique pattern for identification [26]. Their research was also supported by Dr. Paul Tower who published a paper dealing with the study of twins in 1955 [8]. He found out that retinal vessels pattern gives the lowest similarity among other biometric patterns also for monozygotic twins. At that time, the idea of recognition based on retinal vascular pattern was relatively timeless.

With the concept of simple fully automated device that is able to acquire a retinal image and verify a user's identity came Robert Hill in 1975 – founder of EyeDentify, Inc., company, and gave immense effort for its development. However, a fully working device was introduced into the market after several years.

In that time, several other companies have been trying to use available medical fundus cameras and modify them for identification purposes. However, these

cameras had several essential disadvantages, e.g., relatively complicated system for the eye and device optical axes alignment, illumination in visible spectrum which was uncomfortable for a user, and, last but not the least, high price of medical fundus cameras.

Another attempt led to using illumination in a non-visible spectrum (infrared). For these rays is an eye almost transparent except the choroid that reflects it back creating blood vessels pattern. Infrared illumination is not visible to human (thus is more user-friendly), and when the eye is illuminated in infrared range, the pupil is not contracted, and thus, it is possible to acquire larger surface of the retina thanks to a wider field of view.

The first working prototype was created in 1981. Camera optical system using infrared illumination was connected to a personal computer for pattern analysis. After intensive testing, an algorithm of simple correlation was chosen as the most suitable. After another 4 years, EyeDentify, Inc., introduced the standalone product EyeDentification System 7.5 into the market which has been able to identify a person based on the retinal image and the PIN code stored in the internal database. The device was performing a circular scan of the retina using low-intensity infrared light resulting in a contrast feature vector. The image was composed from 256 12-bit logarithmic samples reduced into the record of 40 bytes for each eye.

4.2 EyeDentification System 7.5

The development of retinal recognition device was led mainly by EyeDentify, Inc., company. This corresponds also with numerous obtained patents in this field. The first usable retinal recognition device was introduced in 1981. The product was called EyeDentification System 7.5, and continual improvement of the technology for another 5 years was finished by a system with three registration modes, verification, and identification. Functional principle of the device can be divided into three nontrivial subsystems [3]:

- *Picture, obtaining and processing signals* – optical system and camera must be able to capture an image of the retina in digital form that is suitable for the following processing.
- *Comparison* – the program in the device or in the computer extracts key features from the scanned image and compares these with the samples in database.
- *Representation* – every retinal pattern has to be represented in a way that can be quickly compared or saved into the database.

4.2.1 Optical Scanning System

The mechanical construction of an optical device is a complex issue. It is the most important part of the recognition device because the quality of an input image cannot

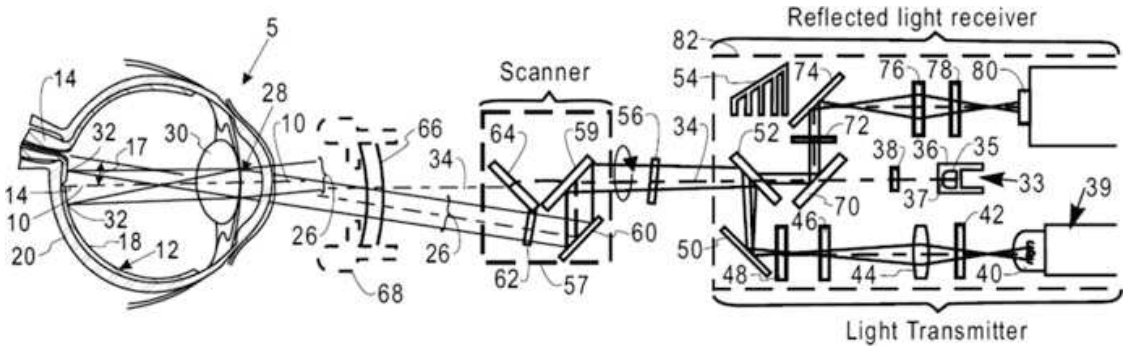

Fig. 3.20 The first version of the optical system used by EyeDentification System 7.5. (From patent US 4620318)

be increased by the following processing in any way, or it is minimally very difficult to enhance the quality. It is evident that the scanning device works on a principle of medical optical devices for eye examination. These so-called retinoscopes or fundus cameras are relatively complex devices, and that is reflected in their price.

Its principle is still similar to retinoscope where a light beam is focused on the retina and a reflected light is captured by a CCD camera. Retinoscope's light beam is set so that the eye lens focuses it as a point on the retinal area. The focused part reflects a part of the sent-back light beam to the eye lens, which modifies it again; the light beam leaves the eye under the same angle as when entering eye (reversible image). By this way, it is possible to get an image of the eye surface about 10° around the visual axis.

First products of the company EyeDentify, Inc., were using a relatively complex optical system with rotary mirrors for covering the scanned area on the retina. This system is described in a patent US 4620318 "Fovea-centered eye fundus scanner" from 1983. The device was performing a circular retinal scan, mostly because of the light reflection from the cornea, where points in the middle would be unusable if raster scanning was used. To balance scanning and visual axis, so-called UV-IR cut filters (hot mirrors reflect infrared illumination but transmit the visible light) and focus point, which the user focuses on, were used. A schematic drawing of the patent can be found in Fig. 3.20. The distance between the eye and optics was about 2–3 cm from the scanner. The system of balancing on an optical axis is a pivotal issue and is described more in detail in patent US 4923297 "Optical alignment system" from 1986.

The newer optical system from EyeDentify, Inc., is much simpler and also has the advantages of optical axis fixation with lower effort of the user needed, compared to the previous system. Its crucial part is the rotary scanning disc, which carries multifocal Fresnel lenses. This construction is described in patent US 5532771 "Eye fundus optical scanner system and method" from 1993.

To ensure that the scanned area is focused on the retina and that the user's eye lies on the scanning beam axis, fixation point/target, on which the user focuses his eye and which must stay in approximately same position for whole scanning, is used. That can be a series of optical networks with focal lengths of −7, −3, 0, and +3

diopters. It is assumed that the most users will be able to focus regardless of their optical defect. When the eye focuses on the target, the device is automatically balanced into the axis of the centered rotary disc on the eye fundus. If the user aligns two or more fixation patterns in one axis, infrared beam is centered on his pupil, and the information can be read.

4.2.2 Comparison

Whenever the user is looking into the optical system's scanning camera, his head can be rotated slightly from the original scanned position during enrollment. Rotation algorithm (phase corrector) is capable of rotating the data by few degrees. This process is done multiple times until the best possible match is reached (highest correlation).

Comparison of obtained samples is done in a few following steps:

- Using sampling the reference, eye record is transformed into the area with the same number of elements as the obtained area, which ensures the alignment (samples overlay).
- Both areas are normalized so that both have RMS (root-mean-square) value equal to 1 – intensities are normalized.
- Areas are correlated using a correlation equivalent to the time domain of the Fourier transformation.

The comparison quality is given by the correlation value where the time shift is equal to zero. It is in a range of +1 (absolute concordance) to −1 (absolute discordance). For a real application, experience has shown that the values around 0.7 can be considered as a concordance.

4.2.3 Representation

Representation of the retina is derived from an image composed out of annular areas (EyeDentification System 7.5 works on the principle of circular scanning). The size of the scanned area is chosen considering the worst possible scanning conditions (highly reduced pupil), but that is still enough for biometric identification. This means that for these purposes, it is not needed to obtain an image of a too large area and resolution.

In relation to the EyeDentify, Inc., device, two main representations of retinal pattern have appeared [27]:

- Original representation has 40 bytes. Those contain information about contrast, coded using real and imaginary coordinates of frequency spectrum generated by Fourier transformation.

- New representation has 48 bytes. It does not contain information about contrast in the time domain. The main advantage of time representation is its faster and more effective processing with lower demands on computing performance.

The template of the retinal pattern contains an area of 96 four-bit contrast numbers from 96 scans of concentric circles in the time domain, i.e., $96 \times 4 = 48$ bytes. Intensities of the time domain can carry a value in interval <−8,7>, while normalization on this resolution is used – adjustment to 4 bits of intensive distribution.

4.3 Characteristics of the Retina Recognition Technology

A selection of characteristics related to the suitability of retinal recognition is listed below.

4.3.1 Acceptability

Compared to the iris recognition in the case of the retina, acceptability is low. Many people are afraid of using this technology. They are convinced that a laser that could cause them an optical defect will be used. These concerns are however absolutely unnecessary because the laser is never used in this case. Another problem is the procedure of getting the retina image itself. It can take longer time depending on the user's cooperation and experience, which could bother some users.

With the retina, direct interaction of the user is also needed (to approach at a distance of few centimeters and focus on fixation points). At least with current methods, relatively big cooperation with the user is necessary. Therefore, the acceptability is really low.

4.3.2 Reliability

Concerning the retina recognition, its reliability is high. However, certain conditions during which it is not possible to obtain the retina picture of appropriate quality do exist. That is, mainly and particularly, unsuitable ambient lighting during which the user's pupil is too contracted. Other problems come with optical defects and eye dysfunctions.

Retina recognition is not very extensive, which may be the reason why not many objective tests of this method exist. In 1991, a multinational company Sandia National Laboratory [28] tested products of EyeDentify, Inc., on hundreds of volunteers. The result was zero FAR and FRR lower than 1%. However, at that time, the testing of biometric systems was in its infancy; therefore, we cannot be sure about the test's objectivity.

According to EyeDentify, Inc., the distribution frequency of each eye's pattern that was compared with any other was getting very close to the ideal Gaussian curve with expected mean value of 0.144 and standard deviation of 0.117 [27]. The corresponding probability in this distribution, expected value, and standard deviation of threshold rating 0.7 is about 1 to million [27].

The method of retina recognition is very prone to certain conditions, which must be kept during every scanning. Conditions which could increase false reject rate are, for example, incorrect distance between the scanner and the eye, unclean optics, edges of contact lenses, and glasses. Ambient lighting can also result in subconscious pupil contraction; for that reason, it is sometimes not possible to use the scanner outdoor during daylight.

4.3.3 Permanence

The biological structure of the retina hardly changes during the lifetime of an individual. However, the recognition can also be influenced by injury of various parts of the eye, e.g., the iris, lens, or other parts limiting outer access to the retinal surface. Retinal blood vessels pattern can also be affected by several diseases like diabetes, glaucoma, high blood pressure, or even heart disease.

4.4 Advantages and Disadvantages of Retinal Technology

From all popular biometrics, the recognition by the retina has the most restrictions. They are not insuperable; however, currently, there is no system that can remove these imperfections on a larger scale. Retinal recognition is also affected by high false reject rate because retinal scanning still requires a relatively high user cooperation which has a tangible impact on the quality of the retinal scan, causing a legitimate user to be rejected.

In comparison with other biometrics, retinal recognition offers relatively high universality, uniqueness, performance, and well resistance against frauds. However, retinal recognition systems are still extremely expensive and less user-friendly.

4.4.1 Advantages

- *Pattern permanence* – retinal blood vessels pattern hardly changes within the lifetime of an individual.
- *Number of unique features* – the rich blood vessels structure can contain up to 400 unique features. Identical twins can also have significantly different patterns.
- *Protection* – the retina is located inside the eye and, thus, is not exposed to threats from external environment. It is well protected and cannot be easily damaged such as fingerprints, hand geometry, etc.

- *Contactless scanning* – sanitary problems are eliminated.
- *Small size of template* – only 96 bytes has a current implementation which is very small in comparison to other biometrics. Thanks to this, it is very suitable for deployment in largely used databases and with a very short processing time.
- *Safety* – the retina is hidden inside the eyeball and is very difficult to acquire a retinal image without user cooperation and awareness. Even though the attacker would know retinal patterns, it is very difficult to imitate the optical system of the eye in order to counterfeit the sensor. After death, the retina degrades very quickly and thus cannot be used in the most cases for accurate postmortem identification.

4.4.2 Disadvantages

- *Fear of eye damage* – low level of infrared illumination used in this type of device is totally harmless for the eye; however, there exists a myth in the general public that these devices can damage the retina. It is required that users are familiarized with the system so that they can trust to it.
- *Outdoor and indoor usage* – a small pupil can increase false reject rate because the light has to come through the pupil twice (once toward the eye, then out of the eye), and the returning light beam can be significantly weakened if the user's pupil is too small.
- *User-friendliness* – the need to approach the eye very close to the sensor and focus the alignment point in the device may reduce the comfort of the device usage more than any other biometric methods. It is also related to sufficiently scanned image quality and using eyeglasses and contact lenses.
- *Strong astigmatism* – people with an optical defect (astigmatism) are not always capable of focusing their eye on a fixation target properly, and thus correct template cannot be generated.
- *High price* – it is expected that the price of the device, especially an optical apparatus for recognition by the retina, will always be higher than, for example, the price of a device for recognition of fingerprint or voice.

4.4.3 Commercial Applications and Devices

Retinal recognition has primarily been used in combination with access control to high-secured areas. This includes facilities such as nuclear development and plants, weapon development and production, government, military, secret organizations, etc. One of the best documented application deployments of retinal recognition was in the state of Illinois which used this technology to prevent welfare fraud by identification of welfare recipients [29]. Considering disadvantages, only a few companies from all over the world have introduced or been developing retinal recognition systems.

Fig. 3.21 EyeDentification System 7.5 [30]

• EyeDentification System 7.5 (EyeDentify, Inc.)
The pioneer in retinal recognition development is EyeDentify, Inc., company, which designed and produced the EyeDentification System 7.5 (Fig. 3.21) and its latest model ICAM 2001, which was introduced in 2001.

According to extant leaflet [29], EyeDentification System 7.5 has been equipped by three modes. Recognition operation mode is the retinal pattern of the user compared with all the eye signature templates stored in a local memory, and a person is allowed or denied depending on existing appropriate template in the database. Second, PIN verification mode: compares the user with only one template identified by a PIN number. The device also allows both eyes verification which reduces the chances of false accepts in PIN mode to one in a trillion. The third mode is enrollment and ensures a proper scan of the retina in order to generate a template and store into database. The user has to keep the eye approximately 15 millimeters above the lens focusing on a green visual alignment target. This process normally takes less than 1 min.

In the PIN verification mode, the recognition process takes approx. 1.5 s. In the recognition mode with 250 retinal templates stored in a local database, the recognition is accomplished in approx. 3 s. The device also provides the following features [29]:

- Stand-alone system or value added component is to increase the security of the currently deployed systems.
- Nonvolatile data storage with capacity of up to 1200 enrollees. The database can be backed up to an external memory.
- System management program control prevents unauthorized users from altering system configuration.
- Average throughput (since first interaction with the device to final acceptance/rejection decision) is from 4 to 7 s.

Fig. 3.22 ICAM 2001 [31]

- RS-232 interface for communication with an external system at a speed of 9600 bits/s or auxiliary port with a speed of 300–19,200 bits/s.
- Dimensions 30.5 × 38 × 20.3 cm.
- The price at product release time was 2500 USD.

• ICAM 2001 (EyeDentify, Inc.)
The last known scanning device produced by EyeDentify, Inc., the ICAM 2001 [31], was pulled out from the market due to its high price. Users found also the ICAM to be somewhat intrusive. The main difference between the older model was mainly in the size of template database (could handle up to 3000 retinal patterns) and also the device was much more compact with a dimension of 23.5 × 15.2 × 10 cm. False reject rate was specified by 12.4% (one try) and 0.4% (three trials).

The company TPI (Trans Pacific Int.) offered also a scanner similar to ICAM 2001. The product was called EyeKey; however, nowadays no information about it is known anymore. According to [32], the design was exactly the same – from this, it can be concluded that the TPI was presenting the ICAM 2001 as its own product with added value in increased user database to 300,000 users and with 15 s comparison time within all stored templates [31] (Fig. 3.22).

• Handheld Retinal Scanner (Retina Technologies, LLC.)
Another manufacturer is, for example, Retinal Technologies, since 2004 known as Retina Systems coming from Boston (US); however, any exact specifications of their system are not publicly available (Fig. 3.23).

One million USD of initial funding was received by Retinal Technologies for the development of an inexpensive way to deploy retinal scanning using a small handheld retinal camera that fits into the palm of the hand [33]. The price was set at just 50 USD only, which is much less compared to the solution of EyeDentify, Inc., company. It was claimed that the scanner uses a patented aspheric lens array capable of capturing a retinal image at distances up to three feet from the user's eye based on ophthalmoscope laser scanning. Templates are stored as codes with length up to 60 bytes. It was also claimed that glasses, contact lenses, and existing medical conditions do not interfere with the scanning of the retina. This technology was primarily intended for medical use in hospitals, but its appearance on the security

Fig. 3.23 Handheld retinal recognition device [33]

market was also expected. With the recent information found, Retinal Technologies was looking for another two million USD to market the technology [34]. No further information about this product can be found, and it is very possible that it was a marketing issue only with regard to low price and small dimension of the device totally different from the devices from EyeDentify, Inc.

5 Multimodal Biometric System

In today's world full of security issues, biometrics is an interesting approach. Ideally, the user interacts with a simple interface and in a matter of seconds, the biometric system scans selected biometric characteristic(s) and decides whether the user is allowed to pass or not.

However, such systems are not perfect, and there is always room for improvement. Recently, it has been discovered that a viable course of biometrics may be based on broader use of multi-biometric (multimodal biometric) systems in the future [35] which combine more than one biometric characteristic for evaluation (e.g., such as fingerprint and palm veins), unlike unimodal biometric systems, which use only a single source. The generalized model of a biometric system can be considered as a unimodal biometric system, i.e., such one which uses a single source of evidence for the identification of persons or verification of their identity. In contrast to this model stands a multi-biometric system. As the name suggests, a multi-biometric system uses more than one source of evidence (biometric characteristic) [35].

If designed correctly, such systems can be expected to be more accurate than their unimodal biometric counterparts [36]. Better security counts also among the most

prominent benefits of multi-biometric systems. By using more sources of evidence, the security of such systems can be substantially improved.

In the case of a unimodal biometric system, specifically, the one which recognizes fingerprints, it might be easy to spoof the sensor with a spoof produced from latent fingerprint and cheat even very intricate liveness detection algorithms [37]. The deployment of a multi-biometric system can effectively prevent this risk by requiring another biometric modality. Multi-biometric systems can also help with situations in which unimodal biometric systems are considered to be discriminative. If an individual lacks a particular trait or if a trait is severely deformed so that the sensor cannot acquire it, then such individuals might be able to provide another biometric trait, and thus the system may allow them to enroll.

Another advantage lies in the fact that some biometric characteristics, e.g., voice, can be damaged by a noisy data signal. Multi-biometric systems can remedy this inconvenience by using a supplementary algorithm or a different modality.

Multi-biometric systems can operate faster in environments that necessitate a large database. Using more than one biometric trait as search criteria, a database that contains thousands of entries might be scanned more efficiently. For example, one trait would refine the list of potential candidates for an identity match, while another one could be then used to determine the identity from the reduced list [38].

On the other hand, multi-biometric systems are not without disadvantages. Usually, there are several methods of implementing such a system, and some perform poorer than others with certain biometrics, while others perform better. It is, therefore, important to contemplate the aims of the system and to design it accordingly.

A multi-biometric system usually brings forth the question of additional cost. Not only does the system have to accommodate additional resources such as a sensor or a chip for a surplus algorithm, but the cost of fusion of the acquired data has to be taken into account as well. Any new biometric trait required from users might also cause significant inconveniences. The question that arises from these facts is whether the costs incurred by the aforementioned are outweighed by the overall benefits of the system [35].

5.1 Biometric Fusion

An important aspect of a multi-biometric system is the fusion of gathered information. At a certain point during the recognition routine, it is necessary to merge the data into a single entity before proceeding further.

This in itself poses a significant challenge in the designing phase of a multi-biometric system development. As shown in Fig. 3.24, there are four separate operations that the system performs. At each of them, fusion can generally be introduced into the system.

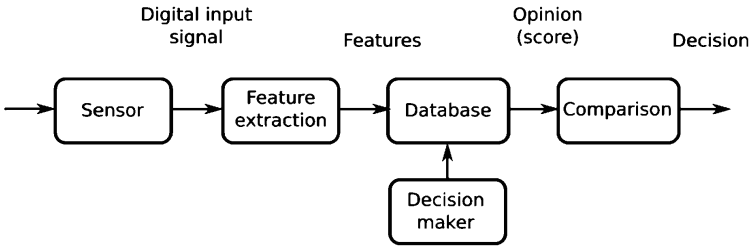

Fig. 3.24 Model of a common biometric system

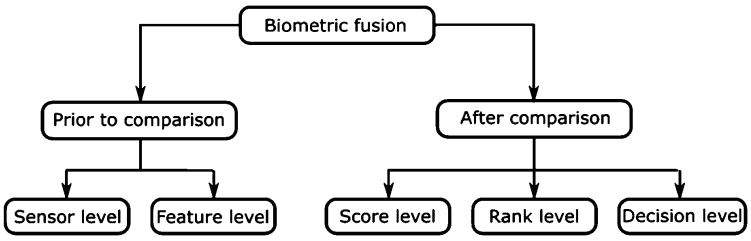

Fig. 3.25 Levels of biometric fusion [40]

It is worth noting that as the data advances through the system, their amount is compressed along the way. However, this does not necessarily imply that the sooner the fusion occurs, the better the results are [39].

While the data at the sensor level are arguably of a larger quantity than those at the feature level, the latter has usually been stripped of superfluous details and noise. On the other hand, it is possible that the feature extraction module may have produced specious results which could have been otherwise remedied at the sensor level.

The classification of biometric fusion is shown in Fig. 3.25.

Biometric fusion can be broadly divided into two sections – *fusion before comparison* and *after comparison*. The reason for this classification results from the fact that after comparison, the amount of information available to the system decreases by a significant margin which is commonly far greater than in the other cases [35].

5.1.1 Sensor-Level Fusion

The sensor-level fusion [41] involves joining multiple sources of raw evidence prior to extracting features. This can encompass text, images, videos, etc. At this level, the obtained data contain the most information available. In image processing, a particular method of fusion is employed, often referred to as mosaicking. In this process, a composite image is constructed from overlapping component images [35].

5.1.2 Feature-Level Fusion

In the feature-level fusion, sources of evidence are consolidated after features have been extracted from respective samples. Following this, fused feature data is then passed to a feature comparator module, and the system proceeds as if dealing with a single source of biometric evidence. Feature sets of distinct modalities or feature sets

of identical modalities that have been extracted by different algorithms pose a challenge for numerous reasons [35]. It may be a problem to fuse two chosen modalities, if the basis on which they should be fused is not known. In these cases, it may be difficult to produce a fused set of features that would satisfy the demands on improvement over a unimodal biometric system. This might be exacerbated by the situation in which feature sets of different modalities are not compatible. One of them may vary in length, while the other one may be represented by a fixed-length set of features [42].

5.1.3 Rank-Level Fusion

It should be noted that the rank-level fusion is only applicable in those biometric systems that are set to identify a person, not to verify his/her identity [43]. It is still one of the more frequently applied methods of fusion. After processing the feature vector and acquiring the comparison score, the set of probable matching identities can be sorted in descending order, and thus, a ranked list of candidate identities can be created. The aim of this level of fusion is to merge the ranks produced by individual biometric modules in order to get a consolidated list of ranks for each identity.

5.1.4 Decision-Level Fusion

The decision-level fusion is particularly useful in situations where two or more finished biometric systems are available, and they need to be combined [41]. More often than not, the decision-level fusion is the only option in this case.

5.1.5 Score-Level Fusion

Score-level fusion is commonly used and preferred in multimodal biometric systems in general because matching scores contain sufficient information making genuine and impostor case distinguishable and are relatively easy to be obtained. Given a number of biometric systems, matching scores for a pre-specified number of users can be generated even with no knowledge of the underlying feature extraction and matching algorithms of each system.

5.2 Bimodal Eye Biometric System

Biometric systems in real-world applications are usually unimodal and thus can handle only one single biometric source of information (biometric characteristic). Unimodal systems are susceptible to a variety of issues such as intra-class variations,

interclass similarities, noisy data, non-universality, and spoofing. By combining the *iris* and *retina* into one solution, it is possible to get very robust biometric recognition. The most important issue of a biometric system is the uniqueness of its biometric information included in the specific biometric characteristic, which influences the strength of such biometric system. The variability in biometric characteristics of the population can be described by biometric entropy. It is also related to a biometric fusion where they could be needed to quantify the biometric information for each biometric characteristic separately and the possible gain from their fusion.

In addition, the anatomic position allows capturing both images at once. An advantage of a bimodal system is also the variability of modes it can operate in. In the case of any requirement for the high secure system, both biometric characteristics can be processed on the same level of protection. In another case, the quality of scanning can be weighted, e.g., if one of these biometric characteristics is evaluated as less reliable (e.g., because of low-quality image acquisition), the second one is preferred if scanned properly. It also leads to a significant improvement of FMR (false match rate) and FNMR (false non-match rate) and higher reliability for the user – if there is no possibility to acquire one of the biometric characteristics for any reason, the system is still able to recognize him/her on the base of the second biometric characteristic.

The bimodal eye biometric system enables to fuse information at the feature level, matching score level and decision level. We identified several current papers addressing the problem of iris and retina fusion. In [44], the score-level fusion of the left and right irises and retinal features is presented. The weighted average of the scores was applied to all possible combinations of the two irises, and equal weights were assigned to each iris. The fused score is then obtained by a linear combination of these two scores. Since two different scores are obtained for the iris and retina, score normalization needs to be performed. Then, the final score is obtained from the scores of fused irises and retinas. Another approach in patent [45] simply attaches both iris and retina codes together. With the mentioned codes, it is possible to perform fusion by logical operations or join them into a bigger one. Several approaches can be used on the image level. For example, we can merge the images and evaluate them (e.g., by Daugman's algorithm). In this case, one of them can be used as a mask for another one, and their mutual relation such as angle or color is then computed.

Nevertheless, the first concept of the simultaneous iris and retina recognition in a single device was published by David B. Usher et al. [46] in 2008. However, the algorithms were not described in detail, and the preliminary results were focused mainly on image acquisition. The first device combining the iris and retina in one single device was introduced as a flagship of eye biometrics by Retica Systems Inc. [47] in 2006. The device is described as a combined hardware and software solution which allows capturing and fusing data from both the retina and the iris, creating the most secure and accurate biometrics in industry. Recognition device called Cyclops was dedicated for high level secured utilization such as border security, facilities, military and defense, nuclear plants, etc. Retica Systems Inc. had a plan of selling hardware or software solution or the software licenses for incorporation into existing

biometric systems. The handheld version has been also supposedly under development. However, the whole project was probably a marketing issue only, because the device codenamed Cyclops had never been introduced and brought to the market [48].

In general, a proposal of ocular biometric device can be divided into four parts:

- *Combined optical system* constructed in order to acquire retina and iris images. In the case of the retina, it is very important to get a sharply focused image and suitable field of view with appropriate surface of the retina. This is related to pupil size and ambient light intensity which must be as low as possible preventing contractions of the pupil. On the other hand, when acquiring an iris image, it is very suitable to have small pupil in order to get the larger surface of the iris. The illuminating light forming bright Purkinje reflections [49] within the iris reflects from the exterior and interior surfaces of the lens and the cornea. These have to be suppressed or restricted out of the region of interest (e.g., restricted to pupil region). Unwanted reflections can be a big problem for any optical system in general and has to be kept at minimum including ambient light sources. Optical system also involves appropriate retina and iris illumination which must be with respect to the pupil size and allowed intensity, preventing the eye from damage.
- *Aligning system* to get the eye optical axis in one line with the optical axis of the device. This is very important when acquiring the retina because the beam of light entering the eyeball is limited by contraction of the pupil, and thus the required field of view is significantly decreasing with the mutual distance of both axes. This applies mainly for retina imaging. The eye and device axes positions must be such that the imaging axis is targeting the surrounding of the blind spot where the most amount of biometric features such as vessels bifurcations or crossings are located. Alignment can be done by two approaches or their combination – the user moves the head toward the device focusing a fixation light point built-in in the device, or the device is moved toward the user's eye depending on the feedback from a camera. Illumination during the process of alignment has also to be comfortable for the user with respect to pupil size as mentioned above. Near-infrared light is usually suitable. Alignment for the iris image acquisition is not so strict, given that the iris can be captured much more easily even from various distances and angles.
- *Image acquisition* – the first step preceding acquisition is an eye localization and identification of boundaries between the iris and the sclera and the iris and the pupil which are not usually concentric. Borders estimation is also related to an identification of areas of the iris that are covered by eyelashes, eyelids, and areas of bright reflections. Several methods have been described initially, based on Daugman's rubber sheet model (see Chap. 3.2.1) [50] or Wildes et al. [51] who also introduced a paper proposal using circular boundary model. Lately, Wildes also presented an algorithm using edge detectors and Hough transforms to segment the eye image, where also, two parabolas were used to find the eyelids. Paper [12] deals with enhanced Daugman's integro-differential method, optimizing its computation time and problem of locating the pupil center outside the

image. The same method is improved in [52] optimized for eye tracking. In a paper [53], it presents an approach for fast iris localization using contrast stretching and leading edge detection. Once the iris is localized and the exact position of the pupil is known, optical axes of the eye and the device must be aligned into one axis. Then it is possible to get an iris image and refocus the optical system to be able to take the retinal image. Focusing on the back of the eye has to be in near-infrared light spectrum to prevent the iris contractions. However, the focus in infrared range can vary against visible spectrum depending on the used wavelength. In other words, the object focused in infrared range is not focused in the visible spectrum and vice versa. It is a property of optical system, but both focuses (infrared and visible) are in mutual correlation shifted by a given constant. At the end of this localization and focusing process, it is finally possible to obtain proper iris and retinal image suitable for recognition itself. Retina and iris image acquisition requires various optical setups and cannot be performed at one time. After the iris image is obtained, it is important to align optical axes of the optics and eye to acquire the retinal image.

- *Image feature extraction and matching* – this is the last step of identification, and in the case of multimodal biometric systems, the extraction is usually followed by some kind of biometric fusion. Features can be joined at different levels of fusion prior to comparison (sensor and feature level) or after the comparison (score, rank, and decision level). Feature extraction and matching methods are described in more detail in previous chapters dealing with appropriate iris and retina biometric.

6 Retinal Features Extraction and Matching

Since the retinal vascular pattern is considered as the main source of biometric features, the first step is usually a segmentation of the vascular tree. The segmentation is followed by the feature extraction, which is based on the detection of bifurcations and crossings of the blood vessels.

Generally, the positions and/or mutual positions of these points, together with some additional features, are used for building a feature vector to cope with translation, rotation, and scale invariants. For example, the work [54] used orientations of blood vessels in specific bifurcation point together with four nearest bifurcations in their feature vector. The Mahalanobis distance gives recognition rate 98.87% for different datasets. In [55], there was defined the so-called principle of bifurcation orientation for each bifurcation, and together with their positions, the point pattern matching method was applied. They achieved total FRR = 4.15% and EER = 1.16% for a database containing 2063 images with small overlap (up to 25%) from 380 subjects diagnosed with diabetes.

One of the main disadvantages of this approach is the detection of bifurcations and crossings using morphological thinning. This step can lead to various results based on the thinning methods. Therefore, the major part of the current approaches

tries to avoid this issue using the whole segmented vascular tree. Eigenvalue analysis of vascularity followed by multi-scale image registration to cope with the spatial transformation between the acquired and template image was introduced in [56]. They achieved 100% recognition rate for their own dataset of 284 retinal images. In [57] sampled binary vascular image along defined lines was used in order to extract binary signals for matching achieving over 95% success on about 400 retinal images. Barkhoda et al. [58] used a skeletonized image of vascularity for feature extraction in specific angular and radial partitions. Application of the fuzzy system with Manhattan distance measure leads to 99.75% accuracy using DRIVE dataset. On the other hand, in [59] there was used original intensity image for extraction intensity profiles along circles centered in the fovea, which must be detected. They achieved an averaged FAR per subject below 0.02 for 58 subjects.

6.1 Optic Disc Localization

Several papers deal with the optic disc localization. For example, [60] uses methods called principal component analysis and gradient vector flow snakes for optic disc borders recognition. This model is very computationally intensive but gives a high accuracy of the blind spot detection. Another approach mentioned in [61] is based on the assumption that an optic disc roughly takes up to 5% of the area of the brightest pixels. This method is very fast. Based on thresholding, it is very important to choose an appropriate threshold value which is computed from the average pixel intensities of background and foreground pixels. However, based on experiments on chosen retinal databases, this algorithm is not very precise.

Another work deals with the detection of the optic disc on an image with high levels of gray [62]. This approach works well if there are no pathologies in the image, which would be bright and very contrasting against the background. The principle of area threshold was used in [63] where disc outlines are detected using Hough transformation. That means that image gradient is calculated and as a disc, an area that corresponds the most to its shape is chosen. The problem of this attitude is that the optical disc does not always possess a circular or elliptical shape in the image. It can be overlapped by vessels that protrude it. The principle of Hough transformation was used also in [63]. Despite some improvements, problems were present while detecting the optical disc when the contrast of the images was too low or when the disc's shape was unconventional. Backward vessel tracing that comes from the optical disc was introduced in [80]. This method is one of the most successful for the localization of the optical disc. Its disadvantage is high resources consumption.

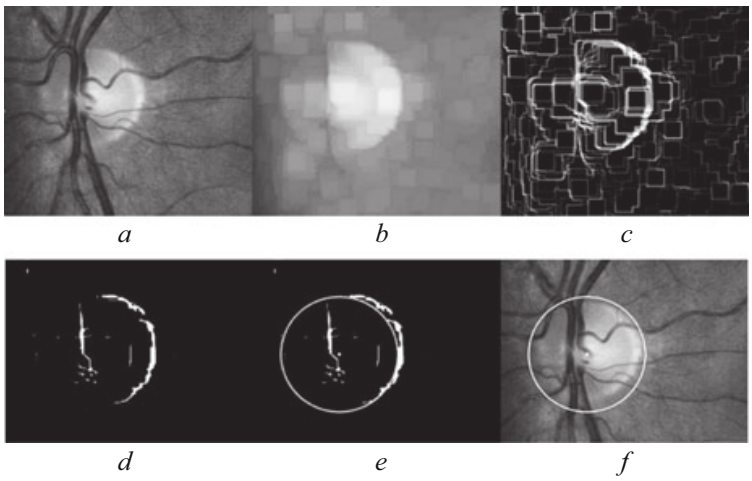

Fig. 3.26 Optic disc localization: (**a**) region of interest; (**b**) removed blood vessels; (**c**) Sobel edge detector; (**d**) eroded binary image; (**e**) Hough circle; (**f**) circle in the original image

6.1.1 Searching Pixels with Highest Average Intensity of Surroundings

This algorithm was inspired by the approach mentioned in [64]. This is based on low-pass filter application (a new pixel intensity value is decided by an average from the surroundings). The pixels of highest intensities are highlighted, and the brightest area is considered as the center of the region of interest (ROI). Subsequent operations are applied to this area only. The following procedures comprise the application of several filters on the ROI and circle detection using Hough circle transformation [65].

The morphological dilatation and Gaussian blur remove blood vessels from the ROI which may have a negative impact on edge detection. Then Sobel edge detector is used, and subsequently an image is converted to a binary form, using thresholding. Noise reduction is performed by morphological erosion. In the last step, Hough transformation is used for the optic disc circle detection. The result is the optic disc center and also its diameter. An example of the whole procedure is shown in Fig. 3.26.

6.1.2 Localization Based on Watershed Segmentation

This approach is based on watershed segmentation described in [66]. Various color specters were compared, red (RGB) channel comes out as the most effective for the detection of the optic disc outlines, where its outlines are the most continuous and also the most contrast to the background. Since that channel has a very small dynamic range and also since the optical disc belongs to the brightest objects in the image for the detection, it is better to use a brightness channel from the HSV model. For disc localization, the variation of gray level is used. As the optic disc is a bright visual object and vessels appear to be dark in the image, the gray level in papillary areas is higher than in other image areas. That is true only if no disease symptoms or other bright artifacts are present on the dark background. That can be addressed by using a shading corrector. In the image with the gray adjustment, the

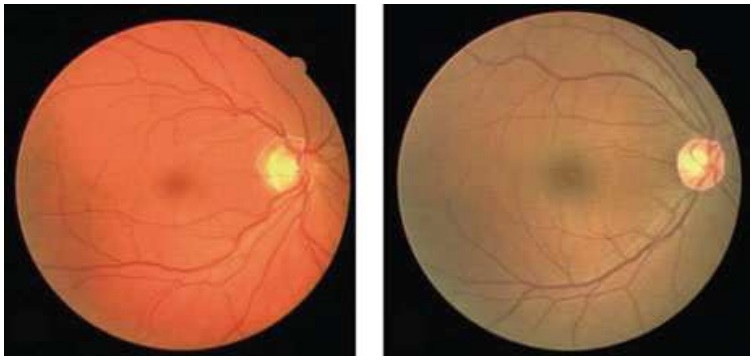

Fig. 3.27 Highlighted optic disc in fundus images

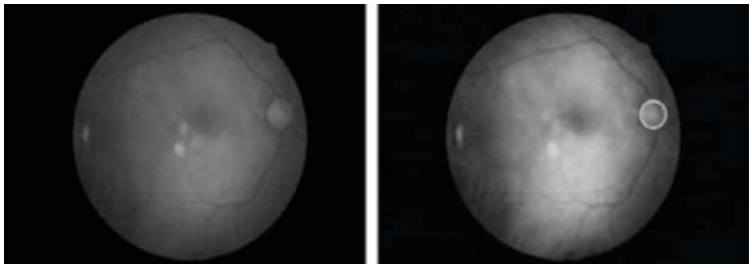

Fig. 3.28 Red channel of the retina image (left), filtered image with optic disc detected (right)

local variation for each pixel is calculated. The global maximum in this adjusted image is situated in the pupil or next to it, which makes it easier to work with a subset of pixels cut from the original picture which does not contain exudates which could disrupt the optical disc detection. Vessels which could distort the result are eliminated before the watershed segmentation [67] for finding the outlines of the optical disc is used. Then the watershed segmentation is used, and its result is the optic disc outline. The result can be seen in Fig. 3.27. The left image shows partial detection only; the highlighted region overlaps its border. The correctly localized optical disc and the borders of the optical disc corresponding to the borders of the highlighted region are shown in the right image.

6.1.3 CLAHE and Median Filter

The red color channel of the original image is used, because the optic disc is the most conspicuous there. Such image is processed by CLAHE [68] and median filter, then the Canny edge detection is performed, and Hough circle transformation [65] is used to detect the optic disc. An example is depicted in Fig. 3.28.

6.2 Fovea Localization

In literature, various approaches for macula detection exist. In [69], principle based on macula outlines detection was introduced with subsequent optimization using ant colony algorithm. The principle from [70], in which it is first necessary to localize

the middle of the optic disc and vascular bed, was also introduced. Then the position of the macula is detected based on the distance from the middle of the optical disc. Thanks to thresholding combined with the obtained mask of the vascular bed, the darkest pixels in the candidate area are searched. Another approach from [71] uses a multilevel thresholding without the need to detect the candidate areas on the retina to detect the macula.

6.2.1 Anatomical Based Approach

Described fovea detection is based on anatomical characteristics of the eyeball, mentioned in [72]. It is based on the assumption that the angle of the optic disc center and the fovea joint is between $-6°$ and + 3° from the horizontal line. Their distance roughly corresponds to double of the optic disc's diameter. This defined sector is used, and the rest of the image is marked by the white color. This approach requires the optic disc diameter and position.

The whole procedure comprises a few steps. The ROI is chosen by the sector-shaped area given by the angle, center, and distance of the optic disc. The rest of the operations are similar to the optic disc detection described in Chap. 6.1.1. The low-pass filter is applied on the ROI, and the lowest intensity pixels are marked (the fovea is darker than the retinal background). Then the fovea is marked as a center of the largest detected area.

6.2.2 Multilevel Thresholding-Based Approach

The algorithm is characterized by low time consumption, and that is one of the reasons why it was also used. The suggested algorithm for the macula detection uses the principle of multilevel thresholding and localizing of ovals through all the image levels. The described approach was inspired by [71].

In the first step, the red channel is extracted from the RGB image because it contains less information than the other channels about vessels and veins in the retina, which can negatively influence the results of ellipse detection. The macula normally does not have a circular or oval shape, and its circumference is often irregular. For preprocessing, a blurring filter is used. Then the resulting image of the retina is segmented in a cycle, where each iteration means limit value increased by one during thresholding. The result of one iteration is shown in Fig. 3.29. This way, thresholding runs throughout all 256 levels, as the retina image in this stage is like a gray picture with 8-bit information for each pixel. By analysis of the resulting images, it has been discovered that threshold values from 100 to 230 have results that possess the most information about the macula position and thus are the most appropriate for the next step, during which ellipses are being searched in final particular images.

The outlines of ellipses are being searched throughout all thresholding levels. All found ellipses from all threshold levels are saved for further processing. Before that,

Fig. 3.29 Red channel of the retinal image after thresholding

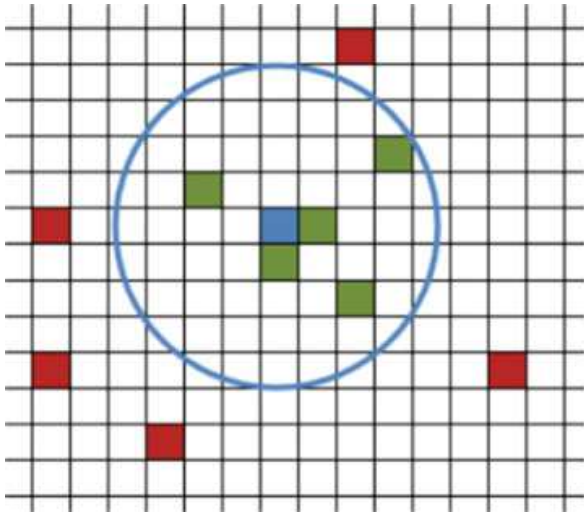

Fig. 3.30 Ellipses clustering

ellipses that do not fulfill the condition that their eccentricity must be larger than 0.5 and simultaneously smaller than 1.5 are removed. Eccentricity is calculated from a rectangle (defined by Eq. (3.5)), which bounds the ellipse with the width (w) and height (h) of this rectangle. The elimination of these inconvenient ellipses is important for removing of misleading areas because the shape of the macula is either a circle or an ellipse with a small eccentricity. On thresholding levels, the blurring filter is used again.

$$exc = \frac{\sqrt{w^2 - h^2}}{w} \tag{3.5}$$

This is done in order to highlight the round shape of areas on the image. Clustering of found ellipses by their center of gravity is depicted in Fig. 3.30. The blue pixel is the group's center of gravity; the green pixels are the ellipses' centers of gravity that belong to the group, and the red pixels are the centers of gravity of ellipses that do not belong to the group [71].

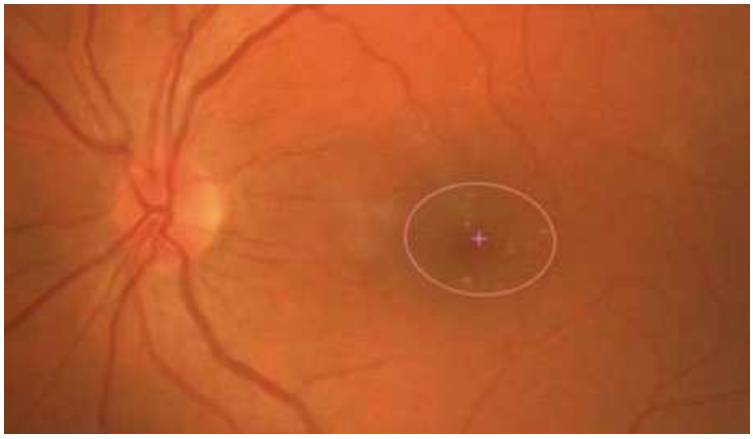

Fig. 3.31 Result of the macula detection in a fundus image

The last part of the macula detection algorithm consists of all the found ellipses. In the beginning, one group for all ellipses is created, and its center of gravity is the same as the center of gravity of the first ellipse. All ellipses are added to this group. Subsequently, all ellipses are shuffled in cycles. If the distance of the shuffled ellipse's center of gravity to the group's center of gravity to which it belongs is bigger than the chosen threshold, a new group is created. To this newly created group, the ellipse is added, and its center of gravity is selected as the group's center of gravity. When all ellipses go through this process, for each group, the center of gravity is calculated as the average center of gravity of all ellipses that belong to the group.

After this recalculation, all ellipses are evaluated again, and if their center of gravity is too far from the group's center of gravity and the found area of the macula circumscribes an ellipse, they are moved to another group, or a new group is created for them. That is repeated until no ellipse has to be moved between groups during the evaluation cycle. As the macular area, the biggest ellipse from the group is chosen. The fundus image with marked macula is shown in Fig. 3.31.

6.3 Blood Vessels Segmentation

The basic approaches for blood vessels detection may be divided into two groups – based on morphological operations and based on 2D filter applications realized by different methods such as matched filters [73], Gabor waves [74], etc. Segmentation in the first group is based on morphological operations and is less computationally intensive. For example, in [75] there is described a very fast segmentation using stop-hat operation.

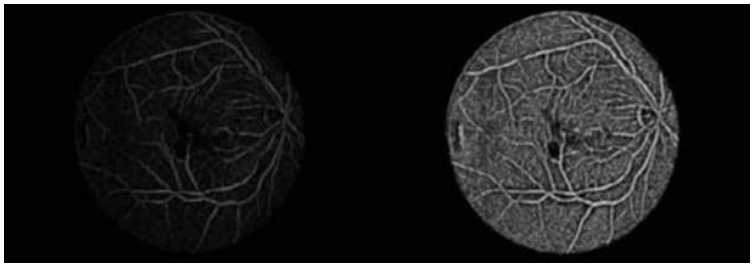

Fig. 3.32 Retinal image before (left) and after (right) thresholding operation

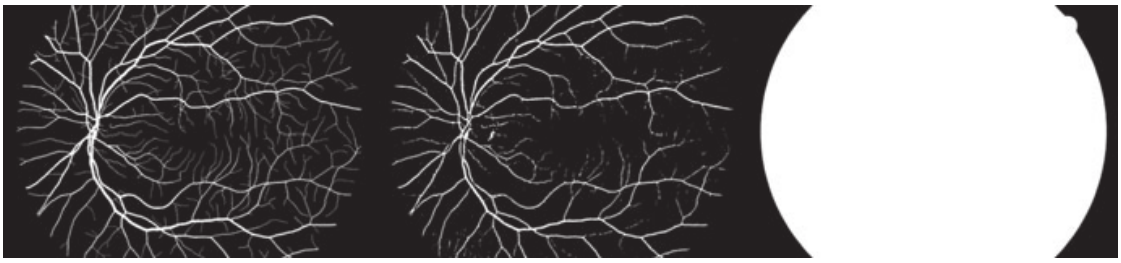

a *b* *c*

Fig. 3.33 Example of the described blood vessels segmentation: (**a**) manually segmented vessels; (**b**) matched filter algorithm used; (**c**) mask of the retinal region in original images

6.3.1 Thresholding

It is desirable to convert an image into a binary form for subsequent processing. This is made by thresholding. The threshold is computed for every input image with the assumption that blood vessels take up approximately 3–10% of the retina image (according to a specific type of imaging device). Another way is the use of adaptive thresholding. However, the main disadvantage of this method is the small white fragments, which are misclassified as vessels.

As shown in Fig. 3.32, not only the retinal veins are highlighted but also the noise which must be removed before bifurcations can be detected. This is achieved by filtering out blobs and by morphological dilatation of the image. This removes small holes and increases the vessels continuity.

6.3.2 Segmentation Using Matched Filter

The described approach is based on the matched filter for blood vessels detection. All the following operations are applied on the green channel of the given image because of higher contrast than in blue or red channel. The whole procedure is depicted in Fig. 3.33.

- *Automatic contrast adjustment* – despite the use of the green channel, blood vessels may have low contrast due to the poor quality of source images. In this case, it is necessary to adjust the contrast. Commonly used methods, such as histogram equalization, are not very suitable in the case of retinal images. The manual contrast adjustment has mostly the best results, but unfortunately, it

cannot be applied in the case where the pictures have to be processed automatically. Inspired by [60], the method called *fast gray-level grouping* gives satisfying results for a given set of retinal images. The principle and implementation details are described in [61]. The main advantage of this method is the fact that the new histogram will have nearly a uniform distribution.

- *Matched filter* – the most important part of the blood vessels detection process is the vessels segmentation from the image background. A 2D filter response, which is defined by Eq. (3.6), is used.

$$\mathbf{K}(x,y) = -e^{\left(\frac{x^2}{2\sigma^2}\right)} \; for \;\; y \leq \left|\frac{L}{2}\right| \tag{3.6}$$

L stands for the minimal length of the vessel, where it does not change its orientation, andσ is the standard deviation in Gaussian (normal) distribution. The exact procedure of the filter generation is based on [76]. The obtained filter is 12 times rotated (each time for 15°), and all the 12 filters are applied on an image. Their responses are added together with their weight resulting in the final response.

6.3.3 Segmentation Using the Difference Between the Filtered Image and the Original

This method of segmentation has been found as the most suitable for the following fusion, thanks to its accuracy and computing speed.

- *Image enhancement* – the input image is enhanced by using the smoothing filters in order to reduce the noise and make the vasculature more visible. In order to obtain the most salient information from the image, the green channel is selected for further processing where the contrast is adjusted by using the contrast-limited adaptive histogram equalization algorithm [77]. This algorithm differs from the simple histogram equalization by calculating histograms for partitions of the image and is added in order to reduce the amplification of the noise inherent to adaptive histogram equalization.
- *Blood vessels detection* – the difference between the filtered image and the original, along with adaptive thresholding, is used to segment the blood vessels. The preceding step for segmenting the veins is the application of the median and blurring filters. This produces a relatively smooth image which is then compared with the non-filtered one. The differential image that results from this comparison is calculated according to the Eq. (3.7):

$$\text{diff}(x,y) = \frac{255}{\max}(\text{original}(x,y) - \text{filtered}(x,y)) \tag{3.7}$$

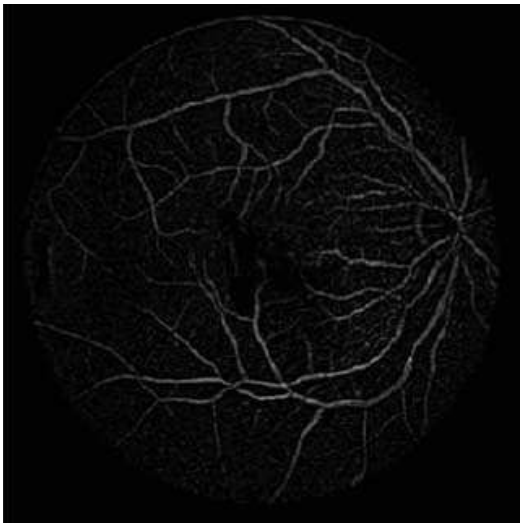

Fig. 3.34 Obtained differential image

where max is the maximum value of intensity difference of the pixels. Although the vascular structure is visible at this point, there is a significant level of noise, and the veins need to be segmented perfectly. The result of this method can be seen in Fig. 3.34.

6.3.4 Thinning

It is essential that thinned vessel must lie strictly in the middle of the original vessel. The simple but fast and well-working algorithm comes from [50]. The thinning is executed from four directions to ensure the position of thinned vessels in the middle of the original one. The algorithm can be described in accordance with [78] as follows:

7 While Points Are Deleted Do

(a) For all pixels $p(i, j)$ do:

If $2 \leq B(P_1) \leq 6$.
$A(P_1) = 1$
$P_2 \times P_4 \times P_6 = 0$ in odd iterations, $P_2 \times P_4 \times P_8 = 0$ in even iterations
$P_4 \times P_6 \times P_8 = 0$ in odd iterations, $P_2 \times P_6 \times P_8 = 0$ in even iterations

(i) Then delete pixel $p(i, j)$.

where $A(P_1)$ is the number of 0 to 1 transitions in a clockwise direction from P_9 back to itself and $B(P_1)$ is the number of non-zero neighbors of P_1. The result of thinning algorithm is depicted in Fig. 3.35.

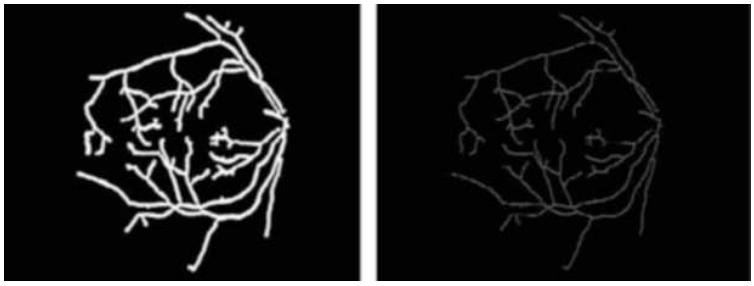

Fig. 3.35 Segmented blood vessels (left) after the thinning operation (right)

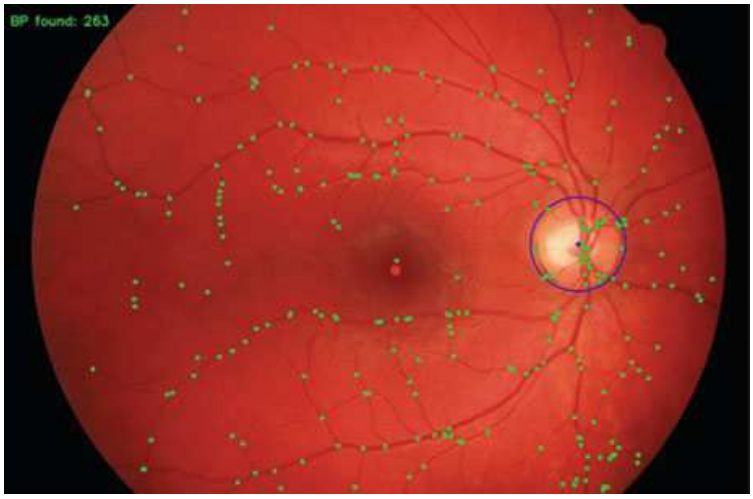

Fig. 3.36 Automatically detected bifurcations in an original image also with the optic disc and fovea

7.1 Bifurcation Localization

Bifurcations are obtained by evaluating every white pixel and its immediate neighborhood. If a bifurcation is to be marked, there must be at least three separate paths that diverge from a given pixel. To calculate this, the neighborhood is analyzed for the number of white pixels and their continuity. If three or more separate white areas are detected, the algorithm regards that pixel as a bifurcation and marks it and stores it in a list of points. If thinning yields an imperfect image with clustered bifurcations, the algorithm has to filter out such bifurcations. The only problem may be caused by the short pieces at the ends of the vessels created as a side effect of thinning. This problem is solved by the definition of a minimal length of the whole three vessels coming out from the point (Fig. 3.36).

7.1.1 Feature Comparison

The comparison module takes two feature vectors. The position of the optic disc is utilized to align bifurcations before image comparison. The adjusted vectors are compared, and the respective score is calculated in accordance with the level of similarity. The score is normalized so that it falls within the interval <0, 1> where a higher value indicates a better match.

First, the two vectors have to be aligned before comparison. This is achieved by taking the optic disc centers and translating the bifurcation points of one image. Since the rotation or angular displacement of images is minimal, only the translation is taken into account.

Next, the similarity score needs to be calculated. The algorithm is as follows:

1. For every bifurcation point b_1 in the smaller array of bifurcations B_1.
   (a) For every bifurcation non-matched point b_2 in the larger array of bifurcations B_2.
      (i) If Euclidean distance between b_1 and b_2 is shorter than the *threshold* and is currently the shortest, mark b_2 as selected.
   (b) If there is a match, mark selected b_2 as matched, and increase the number of matched bifurcations n.
2. Calculate the similarity score.

Then the score is obtained accordingly to Eq. (3.8):

$$\text{score} = \frac{2n}{|B_1| + |B_2|} \tag{3.8}$$

8 Iris Features Extraction and Matching

There is a considerable range of articles focused on the iris recognition. One of the first automated iris recognition systems based on the utilization of Gabor wavelet filters was proposed by Daugman [79]. Several leading and most cited articles can be mentioned, just to outline the widely used approaches for the person's recognition based on the iris characteristic [9, 80, 81]. Usually wavelet-based [9, 79] or texture-based [80] methods for iris recognition are utilized. Other well-known approaches adopted discrete cosine transform (DCT) [81] to the iris pattern encoding. Somewhat recently, new methods for iris characteristic have been published in [82–84]. These approaches utilized the key point descriptors like SIFT (*scale-invariant feature transform*) [82] and SURF (*speeded up robust features*) [83] for the description of the local iris image areas. Also, inspired by earlier approaches, a new approach using wavelets and Gabor filters in combination with support vector machine and Hamming distance classifiers was proposed in [84].

The current iris recognition approaches usually achieve classification accuracy more than 99%. In spite of the current methods, they are very precise and reliable (for ideal images); still, some drawbacks concerning image quality and image acquisition do exist.

8.1 Pupil and Iris Localization

The pupil can be localized by applying an appropriate thresholding technique. First, however, a median filter is applied to the image. This step smoothes out the image and eliminates pixels with outlying values, which further helps in the segmentation procedure.

In order to determine the threshold value, the histogram of the image is calculated. In the lower half (the darker part) of the histogram, a pronounced peak can be found. This, together with the surrounding values, mainly denotes the pixels of the pupil. Therefore, the desired threshold has to be found around this peak. The chosen threshold is higher than the value of the peak in the histogram to ensure that the majority of the pixels of the pupil are included.

After thresholding is applied, the largest black area in the acquired image is bound to denote the pupil. Since it is elliptical in shape, detecting its center and radius can be determined simply by seeking its widest areas. The pupil itself is not entirely circular, but it can be substituted by a circle for the sake of simplicity and avoiding computational complexity.

While the pupil and its surroundings were distinguished from each other by a striking shift in the pixel intensity, the outline of the iris was not so distinct. Therefore, a different approach must be adopted. Although the shift in pixel intensity is not so pronounced, it is present nevertheless. To facilitate its detection, the contrast of the image needs to be adjusted. Together with the use of the median filter, this accentuates the current area of interest which is the outer edge of the iris.

While not being as sharply defined as in the case of the pupil, the outer edge of the iris can be detected by searching for places where the pixel intensity changes clearly over a certain distance. Within the input database, as mentioned above, this approximation gives satisfying results; however this method is not always applicable because of poorer quality of some images. To mitigate this issue, a fail-safe method using 1D Haar wavelets is employed. Although the iris is not entirely circular as well, it is still safe to substitute it by a circle. Additionally, the iris and the pupil are not concentric in general, but to make the algorithm faster and simpler, it has been assumed that they actually are.

Combined with the detected points where the edge of the iris is located, the radius of the iris can be calculated, and thus the extraction of the iris from the image is completed. The whole localization procedure is depicted in Fig. 3.37.

8.2 Features Extraction

The approach at this point varies, but in this algorithm, the unrolling of the iris precedes the segmentation of eyelids. For this unrolling, the Daugman's rubber sheet is used. At this point, the rubber sheet is reduced to a rectangular image with the width of 360 pixels.

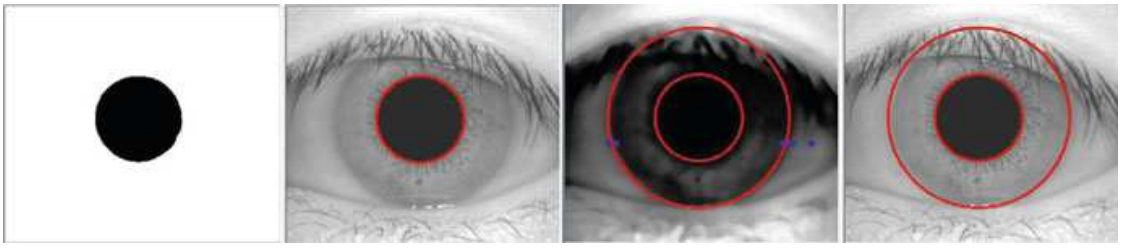

Fig. 3.37 Segmented pupil (left) and the iris. The blue points denote the detected shifts in pixel intensity

Fig. 3.38 Eyelid detection and mask generation. The yellow points denote the borders of examined regions

Eyelids and eyelashes are filtered out by the detector of pixel intensity change along the border of such rectangular image (the stripe). Given the fact that the rough location of the eyelids is predictable, the algorithm defines set boundaries within which the detection is performed. Once the horizontal borders are determined, the algorithm similarly detects the height of the eyelid. When this is done, two masks in the form of tetragons are generated, which have to be taken into account during the final phase of the feature extraction. Of course, this is true only if there are eyelids in the image (Fig. 3.38).

8.2.1 Features Extraction Using Gabor Filter

Gabor filter is represented by the following alternating function:

$$g_{\lambda,\theta,\varphi,\sigma,\gamma(x,y)} = e^{-\frac{(x\cos\theta+y\sin\theta)^2+\gamma^2(-x\sin\theta+y\cos\theta)}{2\sigma^2}} \cos\left(2\pi\frac{x\cos\theta+y\sin\theta}{\lambda}+\varphi\right) \tag{3.9}$$

with the values of wavelength $\lambda = 2$, orientation $\theta = 0°$, phase offset $\varphi = 0$, and aspect ratio $\gamma = 0$.

Before vector quantization, the issue of data reduction has to be addressed. As the height of the stripe can vary (depending on the radius of the iris), the answer to this problem also involves the solution of the issue of potentially varying dimensions of the stripe.

In order to resolve this, certain angular and radial slices of the rubber band are selected for quantization, so that the expected feature vector is of the desired size. During this part, it is necessary to take the eyelid mask into account and map it in accordance with the feature vector. The quantization itself is achieved by using cosine and sine filtering with the resulting vector size of 2048 bits. This represents a 128×8 pixel encoding of the resulting iris stripe, with one real and one imaginary

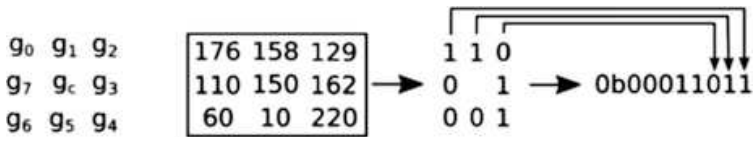

Fig. 3.39 LBP principle

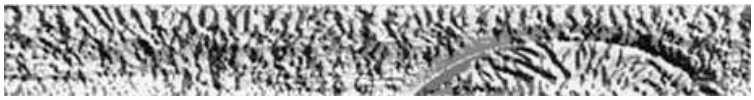

Fig. 3.40 Example of LBP applied on iris image

bit for every pixel. At this point, the feature vector is complemented by a corresponding mask.

8.2.2 Features Extraction Using LBP

The local binary pattern is a method used for classification in computer vision. It is a powerful tool for texture classification first described in [85]. The method describes pixel in the image by a feature vector which is defined with regard to the surroundings [86]. In this case, a basic LBP has been used considering 8-neighborhood.

The LBP is computed by the following method. Each center pixel marked value g_c is compared with 8-neighborhood $g_0 - g_7$, where 0–7 is the index determining the feature position in the resulting vector of size 8 bits (1 byte). The vector value is given by comparison with the pixel in the center. Depending on if the value is smaller or higher, the value in resulting vector is 0 or 1. The base principle of the LBP is depicted in Fig. 3.39.

And from mathematical point of view, it can be expressed by Eq. (3.10):

$$LBP_{P,R} = \sum_{p=0}^{P-1} s(g_p - g_c)2^P, s(x) = \begin{cases} 0, x > 0 \\ 1, x \leq 0 \end{cases} \tag{3.10}$$

where g_p is a value of the surrounding pixel with index p, g_c is a value of the center pixel, P is the surroundings size (in our case 8), and 2^P is a position in the resulting vector. The computed value is then stored on the original position of g_c pixel. Example of the resulting image is shown in Fig. 3.40.

8.3 Features Comparison

Unlike the retinal part, the iris feature comparison is relatively simple. Given two feature vectors, exclusive OR (XOR) operator is applied to the corresponding bits. In this algorithm, if the values are equal, the similarity score is incremented. The masks of respective vectors are used to filter out those pixels which do not include the iris. This reduces the number of pixels to be compared. Thus, the resulting score is normalized so that it fits within the interval between 0 and 1 as depicted in Eq. (3.11).

$$\text{score} = \frac{\text{score}}{2048 - \text{maskedBits}} \tag{3.11}$$

Because of potential differences in the angular position of the input image which were neglected in the feature extraction phase, the score is calculated for several slightly differing angles ranging approximately from $-16°$ to $16°$. The highest score is then selected as the final score and passed on into the decision-making process.

Another but actually very similar approach is to use Hamming distance of two feature vectors according to Eq. (3.12):

$$H = \frac{1}{L} \sum_{j=1}^{L} A_j \oplus B_j \tag{3.12}$$

where L is the size of compared vectors.

9 Eye Livenesss Detection

9.1 Iris

During liveness testing of the iris, a few possibilities are feasible. The most common is the reaction of the iris to lighting changes when the pupil is stretching at lower and contracting at a more intensive light. This reflex is subconscious, and the reaction time is usually between 250 and 400 milliseconds. The pupil contracts and stretches a bit also, under permanent light conditions – this periodical effect is called hippus [19].

Another form of liveness detection can be performed by eye movement or winking according to scanner's voice commands.

Measurement of spectrographic attributes of tissues, fats and blood, are used by more modern devices. Blood reflects very well in the infrared illumination as well as pigment melanin in the iris. This effect is called coaxial back retinal reflection, called the "red eye effect" during photography, where the light is reflected back to a camera if strong light is used.

Purkinje reflexes from the retina and the lens surface can be also used for eye liveness detection. When the outer eye surface is illuminated by an appropriate light source, under certain conditions, an image reflected from the front and back retina surface can appear on the inner surfaces of the eye.

9.2 Retina

Retinal imaging is a relatively difficult process that cannot be easily imitated. To counterfeit that kind of scanner, it would be necessary to use very accurate model of

eye optics with the same attributes as real eye, which is very difficult and almost impossible. Not many information about retina liveness detection exist; however, it is possible to use again medical information, e.g., inanimate retina has a different color. The light reflectivity of the retina or blood flow in blood vessels can be also detected.

Since the eye is a very sensitive organ, we cannot use any invasive method. Reciprocal liveness detection similarly to the iris can be used. However, such detection system could be counterfeit, if after successful liveness detection a real eye is changed for the fake one. For that reason, it is better to test the liveness using various methods. The first method is detecting the color of the macula. By this test, one can find out if the detected eye is living or dissected. Only after death that the macula becomes yellow; until that, it has a reddish color.

Another possibility is liveness detection based on eye movement. A similar principle is used in medicine during eye fundus examination. A medical doctor needs to see the whole retina and not only a part which can be seen from a direct view. Therefore, the device is equipped with a focus point which a patient looks at and toward which he moves the eye so that nearly the whole retina can be seen. This can also be utilized in liveness detection. The device is equipped with a similar focus point and in a few times is randomly moved. During each move, the retina is scanned, and the blind spot or macula position is compared. If the position is varying on each picture, the eye is evaluated as living.

10 Eye Diseases

Every part of our body can be affected by a disease during our lives, whether it is curable or incurable. By incurable disease, we will understand the kind of disability that cannot be eliminated surgically or anyhow else without consequence in the form of loss of biometrical information (e.g., amputation). Curable disease, on the other hand, is removable with minimal consequences (e.g., inflammation, laceration). The retina can be affected by both types of diseases, of course.

For a long time, the eye was an organ that was on the first look dark and untouchable. This started to change in the mid-nineteenth century, thanks to the discovery of ophthalmoscope. Using an ophthalmoscope, it was possible to see the big part of the inner eye. By examination of the eye's background, eye specialists can check the rear part of a patient's eye and determine its health condition. For this eye fundus examination, ophthalmoscope is used. Equipped with rotary lenses, it allows the zooming of individual parts of the retina up to 15 times.

Eye diseases and their potential detection in images play a very important role in biometrics. Unless recognition algorithms are optimized and adjusted, the users suffering from any disease impacting the biometric characteristic cannot fully use an acquisition device or cannot use the technology at all.

Any graphical operation in the retinal images affected by disease may have completely different impact on the result in comparison with a healthy retina. The

number of features correctly detected in image depends on the size of area affected by the disease and on the algorithm ability to recognize features in inhomogeneous environments. Also medical visualization of retinal images is very important for ophthalmologists and can discover diseases related to (hence not only) the eye.

This chapter also describes the most spread diseases of the retina which is much more likely to get sick than the iris.

10.1 Equipment for Retinal Examination

10.1.1 Direct Ophthalmoscope

While using the ophthalmoscope, the patient's eye is examined from a distance of few centimeters through the pupil. Currently, several types of ophthalmoscope are known; however the principle is essentially the same: the eyes of both the examinee and the doctor are on one axis, and the retina is lighted by a light source that incidents on a semitransparent mirror or a mirror with a hole located in the observation axis at an angle of 45° [87]. The disadvantage of a direct ophthalmoscope is the relatively small examination area and the need of skill to operate and also the cooperation of the patient. The field of view (FOV) for this device is approximately 10 degrees. To increase the angle when observing the eye with a direct ophthalmoscope, different approaches can be used. These include placing the device as close to a patient's eye as possible or dilating the pupil. The principle of direct ophthalmoscope is shown in Fig. 3.41. The light beam falls on a small part of the pupil and does not overlap the observing ray, which minimizes the probability of disruptive reflections. The light beam is shown by yellow line; the observing ray is purple.

Complete techniques of ophthalmoscopy were published by a Czech scientist Jan Evangelista Purkinje in 1823. For the following 25 years, many people with miscellaneous specializations were working on creating an ophthalmoscope, but the first usable ophthalmoscope was introduced by Hermann von Helmholtz in 1851. He managed to do it based on the work of Brucke, who however had not been able to explain what the picture of the final rays that enter the observed eye and then come out of it was.

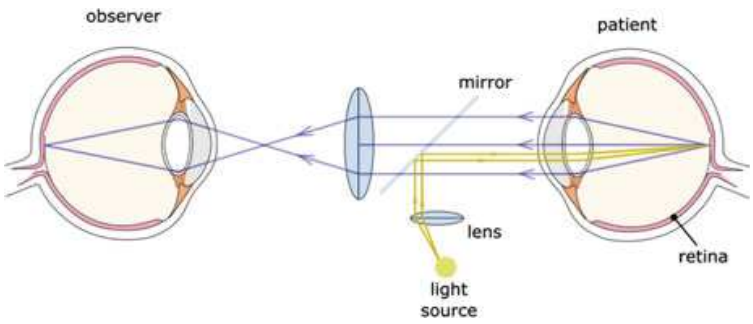

Fig. 3.41 The principle of direct ophthalmoscope [88]

Fig. 3.42 Indirect ophthalmoscopy examination [89]

10.1.2 Binocular Indirect Ophthalmoscope

Most of the important red and yellow details in the retina such as vessels, hemorrhages, or exudates are visible against light red background of blood-filled eye choroid. Subtle and with the naked eye nearly invisible changes can be important symptoms of an ongoing disease. Even better results with direct ophthalmoscope can be achieved with binocular indirect ophthalmoscope [88] that provides a wide field of view, stereoscopic feeling, and also high-contrast resulting image. Logically, this results in other disadvantages – patient's pupil must be dilated, and the device is bigger, heavier, and more expensive. For patients, the most inconvenient is brighter radiation, sometimes even painfully penetrating (Fig. 3.42).

10.1.3 Fundus Camera

For more in-depth examination of the back part of the eye, fundus camera, which has currently and probably the greatest significance in retinal examination, is used. It allows creating a colored photography of nearly whole retinal surface. The optical principle of this tool is based on the so-called indirect ophthalmoscopy [90]. Fundus cameras are usually equipped with a source of white light, which they use to illuminate the retina and then scan it using CCD sensor. Some types can also find the middle of the retina and focus on it automatically using frequency analysis of the scanned image.

This device is usually described by maximal degree, under which it is possible to detect the light reflected from scanned ocular apparatus angle of view. The angle of 30°, which is considered as a standard angle of view, captures the image of an object 2–5 times bigger than it really is. Wide-angle fundus camera captures an image

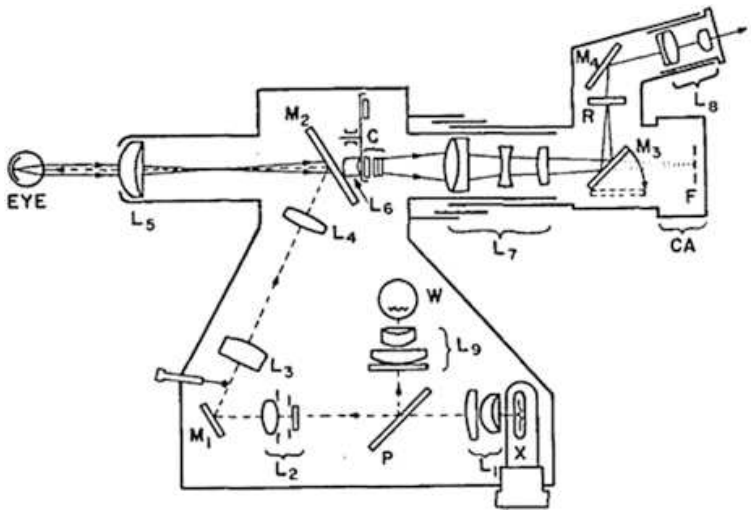

Fig. 3.43 The optical principle of the fundus camera [91]

under the angle of 45°–140°. Depending on the enlargement or reduction of the angle of view, the size of the object that is captured in an image is proportionately changed. Narrow-angle fundus camera uses an angle of view of 20° or less.

The light is generated either by a built-in lamp or using electronic lighting and then projection through a set of filters to a rounded mirror. This mirror reflects light to a group of lenses which focus the light. The mask on the uppermost lens shapes the light into a circle with gross edges. The light is then again reflected from the next round mirror with a central hole, stands out from the camera using lens objective, and continues on to a patient's eye through the cornea. Provided that both lighting systems and image are correctly aligned and focused, the resulting image of the retina stands out from the cornea again back to the device through an unilluminated part of the lens. The light continues through the mirror's central hole to a part of the device for astigmatic correction and to the lenses for dioptric compensation, and a final image is shown on the output lenses of the camera. The optical structure of fundus camera's optics is outlined in Fig. 3.43.

During scanning by the fundus camera, a patient sits in front of the camera's optics with his chin placed on a chin rest and his forehead in a device's forehead rest. The person that is taking the pictures will focus and align the optics to achieve the best possible result. The created photography is then used to determine the patient's diagnosis.

In Fig. 3.44, there is shown an example of the current state of the art of fundus cameras. Canon CR-1 is a non-mydriatic fundus camera with dramatically reduced brightness, improved overall comfort, and significantly shorter exams. One of the advantages of non-mydriatic fundus cameras is that the pupil of the eye does not have to be dilated or enlarged by the use of mydriatic eye drops; thus the examination is more comfortable. For digital imaging, standard DSLR camera is used to obtain a high-quality retinal image with resolution depending on the camera which is used. Canon CR-1 allows wide angle view of 45° and 2× digital magnification. Focusing is performed in two simple steps by aligning two halves of a split pupil image followed in and by the adjustment of split lines and working distance dots in

Fig. 3.44 Canon CR-1 non-mydriatic fundus camera

the retinal display. This ensures that the correct focus and working distance are achieved for the sharp image.

10.2 Macular Degeneration

Macular degeneration is a disease that is in 90% of cases formed with increasing age – then we also talk about age-related macular degeneration (ARMD), and it is the most common cause of blindness for patients over 65 years. It is estimated that more than eight million people in the United States have ARMD in some stadium. With increasing percentage of older people, its presence is still increasing, and it also increases with rising ability to handle other eye diseases. In the rest of the cases, the macular degeneration appears among children or young people in the form of Best disease or Stargardt disease [92]. These diseases are formed based on inheritance.

With macular degeneration, the retinal area that creates the middle of a field of view is damaged. As a consequence, a serious disorder of central field of view emerges. In its middle, a patient sees just gray shadow or even a black spot. The peripheral vision, however, stays unaffected. Macular degeneration can appear in two forms – dry (atrophic) and wet (exudative). Among the most common symptoms belongs blurry gray or black smudge in the center of the field of view (known as central scotoma). An affected person sees deformed straight lines, blurry font, or inappropriate shape of different objects. Color vision is also affected; the colors seem faded. Side vision stays sharp on one or both eyes [92]. An example of a retina affected by macular degeneration is depicted in Fig. 3.45.

Many epidemiologic studies use definition that describes ARMD as degenerative disease of individuals aged over 50, characterized by the presence of one of the following lesions [93]:

Fig. 3.45 Example of macular degeneration with druses

- *Soft (big, $\geq$ 63 μm) druses*. The presence of individual, soft, indistinct druses is considered as a bigger indicator of ARMD than the presence of soft clear druses. The presence of druses with size over 125 μm is also much more important than the presence of smaller druses.
- *Areas of hyperpigmentation* that are associated with druses, with the exception of hard druses surrounded by pigment.
- *Areas of depigmentation* associated with druses. These areas often appear as a shadow of druses and are most often sharply bounded.
- *Visual acuity* is not used for defining ARMD because advanced changes caused by ARMD can be present without changing central fixation.

10.2.1 Druses

This is easily visible as yellowish bearings lying deep in the retina. Druses are distinguished by size and shape, and sometimes they have crystalline look resulting from calcification [93].

As an eye where ARMD is not developed, it is considered that the eye on which no druses are observed or only a few small (smaller than 63 μm), druses with the absence of other ARMD symptoms. An eye in the initial stage of ARMD is one which contains a few (less than approx. 20) middle-sized druses (63–124 μm) or pigment abnormalities (increased pigmentation or depigmentation), without any other symptoms of ARMD. Advanced stage of ARMD is geographic atrophy that interferes into the center of the macula or choroidal neovascularization (CNV). Druses are described by the following characteristics [93]:

- *Types* – druses are generally separated into hard and soft with several subtypes. Soft druses are generally bigger and have a soft look. They have distinct thickness and predisposition to connecting; therefore, they show bigger variation in sizes and types. A cluster of soft druses has a squiggly appearance.

Fig. 3.46 Soft, yellow druses in the inner macula area

- *Degree of eye fundus affection* – this can be evaluated by a number of druses, area of affection, or druses' density which means whether they are separated, touching themselves, or if they cluster together.
- *Distribution* – the greatest importance is attributed to druses that are present in the inner macula, which is defined as an area of inner circle with a diameter of 3000 μm. In Fig. 3.46 can be seen an eye with many clearly visible, soft, yellow druses that are present mainly in the inner macula area.
- *Color* of druses is referred to as yellow, light, or white.

10.3 Diabetic Retinopathy

Diabetic retinopathy (DR) is a noninflammatory disease of eye retina. It is formed as a result of the overall damage of blood vessels during diabetes mellitus [94]. Classification of diabetic retinopathy is generally based on the seriousness of intraretinal microvascular changes and the presence or absence of retinal neovascularization. Retinopathy is classified as non-proliferative diabetic retinopathy (NPDR), if only intraretinal microvascular changes are present. This initial stadium then moves into the proliferative phase, in which new vessels are formed.

Wrongly compensated diabetes affects tiny vessels in the eyes, which are getting blocked, and as a result, the blood supply of the retina is reduced. Another form of retinal damage occurs when blood vessels are leaking and fluid is coming out causing retinal edema. Both insufficient blood supply and retinal edema destroy

the ability to see. The eye tries to correct the situation by growing new blood vessels (neovascularization); however, that substandard and harmful breakup can cause eye extravasation (hemophthalmia) and tractional retinal detachment. Diabetic retinopathy has two forms: non-proliferative and proliferative [95].

Abnormalities of fundus during non-proliferative stage are microaneurysms and intraretinal abnormalities, which are the result of changes in retinal vessels transmittance and eventual blockage of retinal vessels. Vessels' blockage leads to bad blood supplying which appears as an increasing number of hemorrhages, vessel abnormalities, and intraretinal microvascular abnormalities. Retinal hyperperfusion is put in connection with the development of proliferative diabetic retinopathy.

Diabetic retinopathy is characterized by the presence of the following lesions [93]:

- *Microaneurysms of retinal capillaries* – Usually the first visible symptom of diabetic retinopathy. Microaneurysms are ophthalmologically defined as dark red dots with a diameter ranging between 15 and 60 μm. Most often, they are present in posterior areas. Despite that microaneurysms can appear even during other vessel diseases, they are considered to be a typical sign of NDPR. For individual microaneurysms, it is typical that they appear and then disappear with time. Microaneurysms alone without the presence of other symptoms of diabetic retinopathy don't have high clinical importance. In spite of that, the increase of their presence in the retina is connected with the development of retinopathy and increased probability that with their increase, other microvascular changes connected to diabetic retinopathy will appear, exists. In Fig. 3.47, there is shown a very severe diabetic retinopathy. It is characterized by excessive retinal bleeding and also by intraretinal microvascular abnormalities.
- *Hemorrhages* are also red dots that develop as a result of the weakening of microaneurysms' walls or tiny vessels and following the rupture of these walls. Hemorrhages exist in two forms. In the first one, hemorrhages have a character of

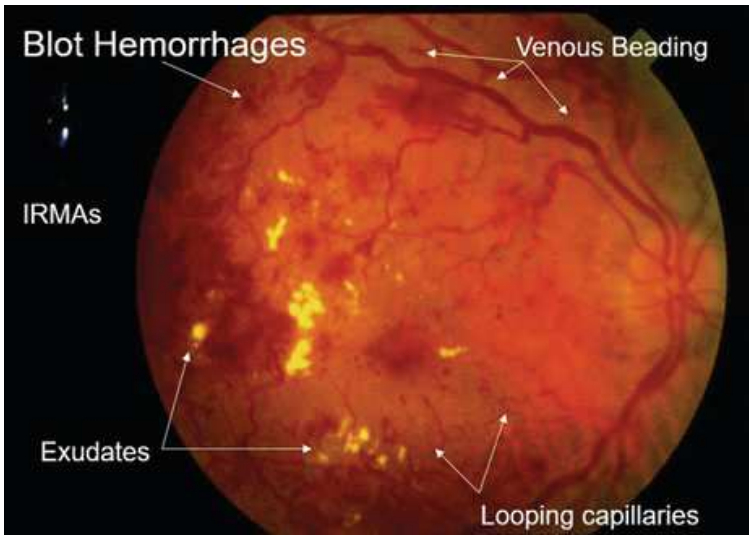

Fig. 3.47 Advanced stage of diabetic retinopathy [96]

dots. These pathologies look like little light red dots. The second type of hemorrhages looks blurry and is bigger.

- *Exudates* – With increased creation of microaneurysms, it is possible that excessive transmittance of retinal capillaries occurs. This leads to the formation of retinal edema, usually in the macular area. Macular edema is defined as the thickening of the retina caused by the gathering of liquid in the macula. Macular edema is often accompanied by hard exudates in the retina. These hard exudates are lipid sediments that are probably piled up under an influence of lipoprotein leak. Clinically, hard exudates are well-boarded, white-yellow intraretinal sediments, normally visible on the edges between edematous and non-edematous retina. The liquid that is creating the edema can come and leave with no visible consequences. Lipid sediments are on the contrary with the liquid connected with the retinal damage and permanent loss of vision, especially if they are located under the center of the macula.

10.4 Toxoplasmosis

Toxoplasmosis is a parasitic disease that ranks among zoonoses, which are diseases transmissible from animals to humans. They appear all over the world. In European countries, about 10–60% of inhabitants have created antibody toward toxoplasmosis, depending on their eating habits. In the Czech Republic, the seropositivity (the presence of antibodies in the blood) is about 20–40%. The disease usually appears only by increased temperature, flu conditions, headaches, fatigue, or swollen lymph nodes. Acute disease can sometimes transform into a chronical stage, often, the infection, however, occurs without any notice and is recognized only by finding specific anti-toxoplasma antibodies in the blood, which can in lower levels last for a whole life (latent phase of infection). A lot of toxoplasmosis' types exist – ganglionic, eye (Fig. 3.48), brain, gynecological, etc. Other forms of toxoplasmosis are not that common [98].

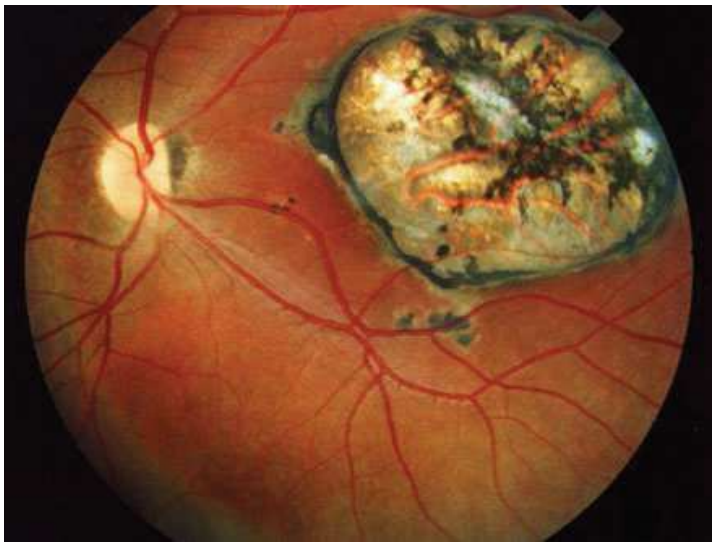

Fig. 3.48 An eye affected by toxoplasmosis [97]

11 Conclusion

In conclusion, we can say that a biometric technology has a big chance of success and is currently displacing conventional non-biometric solutions in many areas. Thanks to combining with cryptographic methods, biometric also penetrates the field of data protection. The field of biometric systems is very alive and still expanding, and innovative solutions that are perfectly usable in industrial applications are coming to the market every year. It can be assumed that even if the eye retina recognition is not currently very popular (there is no retina recognition device currently available in the market), it has undeniable advantages and will evolve and expand. Room for utilization improvement is primarily in high-secured areas such as nuclear plants, military purposes, or secret research laboratories.

Unimodal biometric systems have to contend with issues like non-universality, unacceptable error rates, intra-class variations, etc. Some of these limitations can be solved by the deployment of multimodal biometric systems that integrate the evidence presented by a multiple sources of information. In general, one of the most important issues of a biometric system is the uniqueness of its biometric information included in the specific biometric characteristic, which influences the strength of such system. The variability in biometric characteristics in the population can be described by biometric entropy. It is also related to a biometric fusion and is interesting to see an evaluation of the biometric information for each biometric characteristic separately and the possible gain from their fusion. Multimodal biometric systems elegantly solve several of the problems present in current unimodal systems. By the combination of multiple sources of information, multimodal systems increase population coverage, improve matching performance, and are more resistant against sensor counterfeit. Various fusion levels are possible in multimodal systems.

Acknowledgment This work was supported by the Ministry of Education, Youth and Sports from the National Programme of Sustainability (NPU II) project IT4Innovations excellence in science – LQ1602.

References

1. Wikimedia Commons, *Eyesection.svg*. [Online; accessed 5-July-2016]. URL: https://upload.wikimedia.org/wikipedia/commons/thumb/f/f5/Eyesection.svg/2000px-Eyesection.svg.png
2. D. Roberts, *Anatomy of the Eye. MD Support*, (2013), [Online; accessed 5-July-2016].URL: http://www.mdsupport.org/information/99-2
3. K. Franklin, P. Muir, T. Scott, L. Wilcocks, P. Yates, *Introduction to Biological Physics for the Health and Life Sciences* (Wiley Blackwell, 2010). ISBN 978-0470665930
4. Wikimedi Commons, *File:Retina.svg*. [Online; accessed 5-July-2016] https://commons.wikimedia.org/wiki/File:Retina.svg
5. Z. L. Stan (ed.), *Encyclopedia of Biometrics* (Springer, 2009). ISBN 978-0-387-73003-5

6. L. Yang, *Iris/Retina Biometrics*. CPSC 4600@UTC/CSE, [Online; accessed 5-July-2016]. URL: http://web2.utc.edu/~djy471/documents/b6.1.IRIS-Retina-utc.ppt
7. R.P. Moreno, A. Gonzaga, Features vector for personal identification based on Iris texture, in *Proceedings of the Irish Machine Vision and Image Processing Conference*, (Dublin, 2004)
8. P. Tower, The fundus oculi in monozygotic twins: report of six pairs of identical twins. A.M.A. Arch. Ophthalmol. **54**, 225–239 (1955)
9. J. Daugman, How iris recognition works, in *Proceedings of 2002 International Conference on Image Processing*, vol. 1, (2002)
10. M. Tistarelli, S.Z. Li, R. Chellappa, *Handbook of Remote Biometrics: For Surveillance and Security* (Springer, 2009). ISBN 978-1-447-12670-6
11. J. Daugman, How iris recognition works, in *IEEE Transactions on Circuits and Systems for Video Technology*, vol. 14, no. 1, (2004), [Online; accessed 5-July-2016]: URL: https://www.cl.cam.ac.uk/~jgd1000/csvt.pdf
12. R.B. Dubey, M. Abhimanyu, Iris localization using Daugman's intero-differential operator. Int. J. Comp. Appl., **93**, 6–12 (2014)
13. M. Adam, F. Rossant, F. Amiel, B. Mikovicova, T. Ea, Reliable eyelid localization for iris recognition, in *Conference: Advanced Concepts for Intelligent Vision Systems, ACIVS 2008*, (2008). https://doi.org/10.1007/978-3-540-88458-3_96
14. T. Johar, P. Kaushik, Iris segmentation and normalization using Daugman's rubber sheet model. Int. J. Sci. Tech. Adv. **1**(3) (2015). ISSN: 2454-1532
15. D.D. Zhang, *Automated Biometrics: Technologies and Systems* (Springer, 2013). ISBN 1461545196
16. A. Kumar, *Biometric Security: Iris Recognition*. [Online; accessed 10-August-2015] URL: http://www.slideshare.net/piyushmittalin/biometric-security-iris-recognition
17. J. Daugman, *Results from 200 Billion Iris Cross-Comparisons*. University of Cambridge, Technical report, (2005), ISSN 1476–2986. URL: https://www.cl.cam.ac.uk/techreports/UCAM-CL-TR-635.pdf
18. P. Khav, *Iris Recognition Technology for Improved Authentication*, (SANS Institute, SANS Security Essentials (GSEC) Practical Assignment, 2002), [Online; accessed 5-July-2016]. URL: https://www.sans.org/reading-room/whitepapers/authentication/iris-recognition-technology-improved-authentication-132
19. H. Bouma, L. Baghuis, Hippus of the pupil: periods of slow oscillations of unknown origin. Vis. Res., 11 (11), 1345–1351 (1971)
20. I.D. Iris, *El Salvador Sugar Mill Uses Iris Recognition for Time and Attendance*. [Online; accessed 5-July-2016]. URL: http://www.irisid.com/el-salvador-sugar-mill-uses-iris-recognition-for-time-and-attendance
21. Panasonic Corporation, *Iris Reader Access Control, BM-ET200*. [Online; accessed 5-July-2016]. URL: ftp://ftp.panasonic.com/pub/panasonic/cctv/BidSpecs/BM-ET200.rtf
22. ID Travel AG, *Biometric Systems for Secure and Rapid Access: IrisAccess 4000*. [Online; accessed 5-July-2016]. http://www.id-travel.ch/Downloads/FS_IrisAccess_en.pdf
23. IrisID, iCAM D1000, in *An Eye Fundus Scanner*. [Online; accessed 5-July-2016]. URL: http://www.irisid.com/productssolutions/hardwareproducts/icamd1000
24. Iritech, Inc., *IriShield™ Series*. [Online; accessed 5-July-2016]. URL: http://www.iritech.com/products/hardware/irishield%E2%84%A2-series#
25. J.P. Holmes, L.J. Wright, R.L. Maxwell, *A Performance Evaluation of Biometric Identification Devices* (Sandia National Laboratories, 1991). Technical Report SAND91-0276
26. C. Simon, I. Goldstein, A new scientific method of identification. N. Y. State J. Med. **35**(18), 901–906
27. R.B. Hill, *Biometrics: Retina Identification: Personal Identification in Networked Society* (Springer, 2006). ISBN 978-0-387-28539-9
28. J.P. Holme, L.J. Wright, R.L. Maswell, *A Performance Evaluation of Biometric Identification Devices*. Sandia report, SAND91–0276, (1991), [Online; accessed 5-July-2016]. URL: http://prod.sandia.gov/techlib/access-control.cgi/1991/910276.pdf

29. J. Farmer, *Stop All Federal Abuses Now! S.A.F.A.N*. Internet Newsletter, No. 264, (1997), [Online; accessed 5-July-2016]. URL: http://www.iahushua.com/WOI/illinois.htm
30. EyeDentify Inc., *The Ultimate in Positive Identification, EyeDentification system 7.5*. Leaflet, (1985), [Online; accessed 5-July-2016]. URL: http://simson.net/ref/biometrics/Biometrics/1985.Eyedentify.System7.5.pdf
31. Rayco Security Loss Prevention Systems, Inc., *Retina Verification, ICAM 2001, EyeDentify Retina Biometric Reader*. [Online; accessed 5-July-2016]. URL: http://www.raycosecurity.com/biometrics/EyeDentify.html
32. Trans Pacific (GNF) International, Inc., *EyeKey System*. [Online; accessed 5-July-2016]. URL: http://www.tpi-gnf.com/eky1.htm
33. Retinal Technologies, *A Handheld Scanner*. [Online; accessed 5-July-2016]. URL: http://biometrics.mainguet.org/types/eye_retinal.htm
34. C. Holmes, S. Walmsley, *Biometric Security in Today's Market: An Introduction to Fingerprint, Retinal, and Iris Scanning Technologies*. COP4910 – Frontiers in Information Technology, 2005, [Online; accessed 5-July-2016]. URL: http://pegasus.cc.ucf.edu/~cholmes/homepage/Biometrics.doc
35. A.K. Jain, A.A. Ross, K. Nandakumar, *Handbook of Multibiometrics* (Springer, New York, 2006). ISBN 978-038-7331-232
36. L. Hong, Y. Wan, A.K. Jain, Fingerprint image enhancement: algorithms and performance evaluation, in *IEEE Transactions on Pattern Analysis and Machine Intelligence*, (1998), pp. 777–789
37. T. Matsumoto, H. Matsumoto, K. Yamada, S. Hoshino, R.L. Renesse, Impact of artificial "gummy" fingers on fingerprint systems, in *Optical Security and Counterfeit Deterrence Techniques*, (2002), pp. 275–289. https://doi.org/10.1117/12.462719
38. Techbiometric, *Advantages of Multi-biometric Systems Over Unibiometric Systems*. [Online; accessed 5-July-2016]. URL: http://techbiometric.com/articles/advantages-of-multi-biometric-systems-over-unibiometric-systems
39. M. Faundez-Zanuy, L. O'Gorman, A.K. Jain, N.K. Ratha, Data fusion in biometrics, in *IEEE Aerospace and Electronic Systems Magazine*, (2005), pp. 34–38. https://doi.org/10.1109/MAES.2005.1396793
40. S. Paunovic, I. Jerinić, D. Starčević, Methods for biometric data connection in multimodal systems, in *Proceedings of the XIV International Symposium SYMORG 2014: New Business Models and Sustainable Competitiveness*, (2014), pp. 900–906 ISBN 978-8-676-80295-1
41. K. Nandakumar, *Multibiometric Systems: Fusion Strategies and Template Security* (ProQuest, 2008). ISBN: 978-0-549-61747-1
42. A.K. Jain, B. Chandrasekaran, N.K. Ratha, Dimensionality and sample size considerations in pattern recognition practice, in *Handbook of Statistics*, (1982), p. 835. https://doi.org/10.1016/S0169-7161(82)02042-2
43. N. Radha, A. Kavitha, Rank level fusion using fingerprint and iris biometrics, in *Indian Journal of Computer Science and Engineering*, (2012), pp. 917–923
44. L. Latha, S. Thangasamy, A robust person authentication system based on score level fusion of left and right irises and retinal features, in *Proceedings of the International Conference and Exhibition on Biometrics Technology*, vol. 2, (2010), pp. 111–120. https://doi.org/10.1016/j.procs.2010.11.014
45. D.F. Muller, G.L. Heacock, D.B. Usher, *Method and System for Generating a Combined Retina/Iris Pattern Biometric*, US Patent 7248720, (2007)
46. D. Usher, Y. Tosa, M. Friedman, Ocular biometrics: simultaneous capture and analysis of the retina and iris, in *Advances in Biometrics: Sensors, Algorithms and Systems*, (Springer, 2008), pp. 133–155 ISBN: 1846289203
47. Find Biometrics, *Retica Systems Inc. Announces the World's First Iris-Retina Biometric System*. 2006, [Online; accessed 5-July-2016]. URL: http://findbiometrics.com/retica-systems-inc-announces-the-worlds-first-iris-retina-biometric-system

48. PR Newswire, *Retica Systems Inc. Announces the World's First Iris-Retina Biometric System*. News 2006, [Online; accessed 5-July-2016]. URL: http://www.prnewswire.com/news-releases/retica-systems-inc-announces-the-worlds-first-iris-retina-biometric-system-55935287.html
49. A. Jóźwik, D. Siedlecki, M. Zając, Analysis of Purkinje images as an effective method for estimation of intraocular lens implant location in the eyeball. Optik Int. J. Light Electron Opt. **125**(20), 6021–6025 (2014). https://doi.org/10.1016/j.ijleo.2014.06.130
50. J.G. Daugman, *Biometric Personal Identification System Based on Iris Analysis*. US Patent 5291560, (1994)
51. R.P. Wildes, J.C. Asmuth, K.J. Hanna, S.C. Hsu, R.J. Kolczynski, J.R. Matey, S.E. McBride, A*utomated, Non-invasive Iris Recognition System and Method*. US Patents 5572596 and 5751836, (1996)
52. M. Barbosa, A.C. James, Joint iris boundary detection and fit: a real-time method for accurate pupil tracking. Biomed. Opt. Express **5**(8), 2458–2470 (2014). https://doi.org/10.1364/BOE.5.002458
53. I.A. Saad, L.E. George, Robust and fast iris localization using contrast stretching and leading edge detection. Int. J. Emerg. Trends Technol. Comput. Sci. **3**, 61–67 (2014). ISSN 2278-6856
54. S. Qamber, Z. Waheed, M.U. Akram, Personal identification system based on vascular pattern of human retina, in *Cairo International Biomedical Engineering Conference, 2012*, vol. 2012, pp. 64–677 ISBN 978-1-4673-2800-5
55. H. Oinonen, H. Forsvik, P. Ruusuvuori, O. Yli-Harja, V. Voipio, H. Huttunen, Identity verification based on vessel matching from fundus images, in *Proceedings of IEEE International Conference on Image Processing*, (2010), pp. 4089–4092 ISBN 978-1-4244-7993-1, ISSN 1522-4880
56. C. Mariño, M.G. Penedo, M. Penas, M.J. Carreira, F. Gonzalez, Personal authentication using digital retinal images. Springer Pattern Anal. Appl **9**(1), 21–33 (2006). ISSN 1433-7541
57. C. Köse, C. İkibaş, A personal identification system using retinal vasculature in retinal fundus images. Expert Syst. Appl. **38**(11), 13670–13681 (2011)
58. W. Barkhoda, F. Akhlaqian, M. Amiri, M. Nouroozzadeh, Retina identification based on the pattern of blood vessels using fuzzy logic, in *EURASIP Journal of Advances in Signal Processing*, (2011), pp. 113–121 ISSN: 1687-6180
59. H. Borgen, P. Bours, Wolthusen S. D., Visible-spectrum biometric retina recognition, in *Proceedings of International Conference on Intelligent Information Hiding and Multimedia Signal Processing*, (2008), pp. 1056–1062 ISBN 978-0-7695-3278-3
60. G.V. Saradhi, S. Balasubramanian, V. Chandrasekaran, Performance enhancement of optic disc boundary detection using active contours via improved homogenization of optic disc region, in *International Conference on Information and Automation*, (ICIA, 2006), pp. 264–269 ISSN 2151-1802
61. P.C. Siddalingaswamy, G.K. Prabhu, Automated detection of anatomical structures in retinal images. Int. Conf. Comput. Intell. Multimed. Appl. **3**(10), 164–168 (2007). ISBN 0-7695-3050-8
62. S. Tamura, Y. Okamoto, K. Yanashima, Zero-crossing interval correction in tracing eye-fundus blood vessels. Pattern Recogn. **3**, 227–233 (1988). https://doi.org/10.1016/0031-3203(88)90057-x
63. A. Pinz, S. Bernogge, P. Datlinger, et al., Mapping the human retina, in *IEEE Transactions on Medical Imaging, No. 4*, (1998), pp. 606–619. https://doi.org/10.1109/42.730405
64. D.W.K. Wong, J. Liu, N.M. Tan, et al., Automatic detection of the macula in retinal fundus images using seeded mode tracking approach, in *IEEE Engineering in Medicine and Biology Society, Institute of Electrical & Electronics Engineers (IEEE)*, (2012). https://doi.org/10.1109/embc.2012.6347103
65. J. Parker, *Algorithms for Image Processing and Computer Vision* (Wiley Computer Publishing, New York, 1997). ISBN 04-711-4056-2

66. C. Sinthanayothin, J.F. Boyce, H.L. Cook, et al., Automated localization of the optic disc, fovea, and retinal blood vessels from digital color fundus images. Br. J. Ophthalmol. **83**(8), 902–910 (1999). 10.1136/bjo.83.8.902
67. S. Umbaugh, *Digital Image Processing and Analysis: Human and Computer Vision Applications with CVIPtools* (CRC Press., ISBN 978-1-4398-0205-2, Boca Raton, FL, 2011)
68. T. Johar, P. Kaushik, Iris segmentation and normalization using Daugman's rubber sheet model. Int. J. Sci. Tech. Adv. **1**(3) (2015). ISSN: 2454-1532
69. G. Kavitha, S. Ramakrishnan, Identification and analysis of macula in retinal images using Ant Colony Optimization based hybrid method, in *2009 World Congress on Nature & Biologically Inspired Computing (NaBIC), Institute of Electrical & Electronics Engineers (IEEE)*, (2009). https://doi.org/10.1109/nabic.2009.5393783
70. M. Mubbashar, A. Usman, M.U. Akram, Automated system for macula detection in digital retinal images, in *IEEE International Conference on Information and Communication Technologies*, (2011). https://doi.org/10.1109/icict.2011.5983555
71. D.W.K. Wong, J. Liu, N.M. Tan, et al., Automatic detection of the macula in retinal fundus images using seeded mode tracking approach, in *IEEE Engineering in Medicine and Biology Society, Institute of Electrical & Electronics Engineers (IEEE)*, (2012). https://doi.org/10.1109/embc.2012.6347103
72. P. Verlinde, G. Chollet, Comparing decision fusion paradigms using k-NN based classifiers, decision trees and logistic regression in a multi-modal identity verification application, in *Second International Conference on Audio and Video-Based Biometric Person Authentication*, (2003)
73. S. Chaudhuri, S. Chatterjee, N. Katz, M. Nelson, M. Goldbaum, Detection of blood vessels in retinal images using two-dimensional matched filters, in *IEEE Transactions on Medical Imaging, No. 3*, (1989), pp. 263–269 ISSN 0278-0062
74. B. Jähne, *Digital Image Processing Concepts, Algorithms, and Scientific Applications* (Springer, Berlin Heidelberg, 1997). ISBN 978-3-662-03479-8
75. A. Aquino, M.E. Gegúndez, D. Marín, Automated optic disc detection in retinal images of patients with diabetic retinopathy and risk of macular edema, in *World Academy of Science, Engineering and Technology, No. 60*, (2009), pp. 87–92
76. J. Parker, *Algorithms for Image Processing and Computer Vision* (John Wiley & Sons, 1996). isbn:0471140562
77. P.S. Heckbert, *Graphics Gems IV*, Graphic Gems Series (AP Professional, 1994). ISBN 0-12-336155-9
78. N. Dede, *Implementation of Thinning Algorithm in OpenCV*. OpenCV Code, [Online; accessed 5-July-2016]. URL: http://opencv-code.com/quick-tips/implementation-of-thinning-algorithm-in-opencv
79. J.G. Daugman, High confidence visual recognition of persons by a test of statistical independence. IEEE Trans. Pattern Anal. Mach. Intell. **15**(11), 1148–1161 (1993). ISSN 0162-8828
80. L. Ma, T. Tan, Y. Wang, D. Zhang, Efficient iris recognition by characterizing key local variations. IEEE Trans. Image Process. **13**(6), 739–750 (2004)
81. D.M. Monro, S. Rakshit, D. Zhang, DCT-based iris recognition. IEEE Trans. Pattern Anal. Mach. Intell. **29**(4), 586–595 (2007). ISSN 0162-8828
82. S. Sun, S. Yang, L. Zhao, Non-cooperative bovine iris recognition via SIFT. Neurocomputing **120**, 310–317 (2013). https://doi.org/10.1016/j.neucom.2012.08.068
83. H. Mehrotra, P.K. Sa, B. Majhi, Fast segmentation and adaptive SURF descriptor for iris recognition. Math. Comput. Modell., Elsevier **58**(1–2, 132), –146 (2013). ISSN: 0895-7177
84. H. Rai, A. Yadav, Iris recognition using combined support vector machine and hamming distance approach. Exp. Syst. Appl. **41**(2), 588–593 (2014)
85. T. Ojala, T. Pietikäinen, D. Harwood, Performance evaluation of texture measures with classification based on Kullback discrimination of distributions, in *Proceedings of the 12th IAPR International Conference on Pattern Recognition*, vol. 1, (1994), pp. 582–585 ISBN 0-8186-6265-4

86. M.Y. Shams, M.Z. Rashad, O. Nomir, M.Z. El-Awady, Iris recognition based on LBP and combined LVQ classifier. Int. J. Comput. Sci. Inf. Technol. **3**(5) (2011). https://doi.org/10.5121/ijcsit.2011.3506
87. J. Macek, *Klasifikace a rozpoznávání patologických nálezů v obrazech sítnice oka (Classification and Recognition of Pathologic Foundings in Eye Retina Images)*. Master's thesis, Faculty of Information Technology, Brno University of Technology, (2015)
88. M. Yanoff, *Ophthalmology*, 3rd edn. (Mosby Elsevier, 2009). ISBN 978-0-323-04332-8
89. Mayo Clinic, *Indirect Ophthalmoscopy*. [Online; accessed 5-July-2016]. URL: http://www.mayoclinic.org/tests-procedures/eye-exam/multimedia/indirect-ophthalmoscopy/img-20006175
90. S.E. Sherman, *History of Ophthalmology: The History of the Ophthalmoscope*, vol 2 (Springer, 1989), pp. 221–228 ISBN 978-0-7923-0273-5
91. R.L. Wiggins, K.D. Vaughan, G.B. Friedmann, Holography using a fundus camera. Appl. Opt. (1), 179–181 (1972). https://doi.org/10.1364/AO.11.000179
92. J. Orellana, A.H. Friedman, *Clinico-Pathological Atlas of Congenital Fundus Disorders: Best's Disease* (Springer, 1993), pp. 147–150., ISBN 978-1-4613-9322-1
93. A.P. Schachat, P. Wilkinson Ch, D.R. Hinton, P. Wilkinson, *Retina*, 4th edn. (Mosby Elsevier, 2005). ISBN 978-0-323-04323-6
94. L. Poretsky (ed.), *Principles of Diabetes Mellitus*, 2nd edn. (Springer, 2010). ISBN 978-0-387-09840-1
95. W. Gloria, *Diabetic Retinopathy: The Essentials*. LWW; 1 Har/Psc edition, (2010.), ISBN 1605476625
96. American Optometric Association, Diabetic eye disease, in *Diabetic Eye Disease*, (2009), [Online; accessed 5-July-2016], URL: http://www.slideshare.net/MedicineAndHealth14/diabetic-eye-disease
97. W. Lihteh, *Ophthalmologic Manifestations of Toxoplasmosis*. [Online; accessed 5-July-2016]. URL: http://emedicine.medscape.com/article/2044905-overview
98. J.D. Camet, H. Talabani, E. Delair, F. Leslé, H. Yera, A.P. Brézin, *Toxoplasmosis – Recent Advances: Risk Factors, Pathogenesis and Diagnosis of Ocular Toxoplasmosis* (Intech, 2012). ISBN 978-953-51-0746-0
99. C. Tisse, L. Martin, L. Torres, M. Robert, Person identification technique using human iris recognition, in *Proceedings of ICVI 2002*, (2002), pp. 294–299
100. H.E. Lahn, *Iridology: The Diagnosis from the Eye* (Kessinger Publishing, 2010). ISBN 978-1162622729
101. M.U. Akram, S. Khalid, S.A. Khan, Identification and classification of microaneurysms for early detection of diabetic retinopathy. Pattern Recogn. **46**(1), 107–116 (2013). https://doi.org/10.1016/j.patcog.2012.07.002.s
102. S. Qamber, Z. Waheed, M.U. Akram, Personal identification system based on vascular pattern of human retina, in *Cairo International Biomedical Engineering Conference, 2012*, (2012), pp. 64–677 ISBN 978-1-4673-2800-5